Chapter 2B. Analysis of Imaging Spectrometer Data for the Aynak-Logar Valley Area of Interest

By K. Eric Livo and M.R. Johnson

Abstract

Imaging spectrometer data of the Aynak-Logar Valley area of interest (AOI) in the central northeastern part of Afghanistan were analyzed to identify the occurrences of selected materials at the surface. Mineral distributions were mapped by comparing spectral features in the pixels of HyMap imaging spectrometer data to reference spectra of minerals and other materials. HyMap data were used to detect areas with the potential for sedimentary-hosted copper and podiform chromite mineralization.

Sedimentary-hosted copper mineralization in the eastern subareas of the Aynak-Logar Valley AOI are hosted in dolomite (marble) and mica-quartz schist that trend to the northeast along structural folds. The copper mineralization trend is detected in these HyMap-derived mineral maps as areas of dolomite associated with igneous intrusives. Western subarea podiform chromite mineralization is hosted within pre-Eocene ultramafic rocks that are mapped in the HyMap data as ferrous and ferric iron-rich serpentine-bearing rocks. Chlorite and (or) epidote are mapped along the ultramafic rock contacts. Areas of dolomite and calcite with goethite occur preferentially in ultramafic-rich Tertiary alluvium and fan deposits. Mineral maps created from the analysis of imaging spectrometer data have revealed terrane that have the potential to host copper and chromite mineralization.

2B.1 Introduction

Previous U.S. Geological Survey (USGS) analyses of existing geologic data of Afghanistan revealed numerous areas with indications of potential mineral resources of various types (Peters and others, 2007). From these areas of interest (AOIs), several were selected for follow-on studies using modern hyperspectral remote sensing data to further characterize surface materials. One area is the Aynak-Logar Valley AOI, within northern Logar and southern Kabul Provinces, about 30 kilometers southeast of the capitol city of Kabul (fig. 2B–1).

2B.1.1 Hyperspectral Data Collection and Processing

In 2007, imaging spectrometer data were acquired over most of Afghanistan as part of the USGS Oil and Gas Resources Assessment of the Katawaz and Helmand Basins project. These data were collected to characterize surface materials in support of assessments of resources (coal, water, minerals, and oil and gas) and earthquake hazards in the country (King and others, 2010). Imaging spectrometers measure the reflectance of visible and near-infrared light from the Earth's surface in many narrow channels producing a reflectance spectrum for each image pixel. These reflectance spectra can be interpreted to identify absorption features that arise from specific chemical transitions and molecular bonds that provide compositional information about surface materials. Imaging spectrometer data can be used to characterize only the surface materials and not subsurface composition or structure. However, subsurface processes can be indicated by the distribution of surface materials that can be detected using imaging spectroscopy data.

To help assess these potential resources, high-resolution hyperspectral data were analyzed to detect the presence of selected minerals that may be indicative of past mineralization processes. This report contains the results of those analyses and identifies numerous sites within the Aynak-Logar

Valley AOI that could merit further investigation, especially detailed geological mapping and geochemical studies.

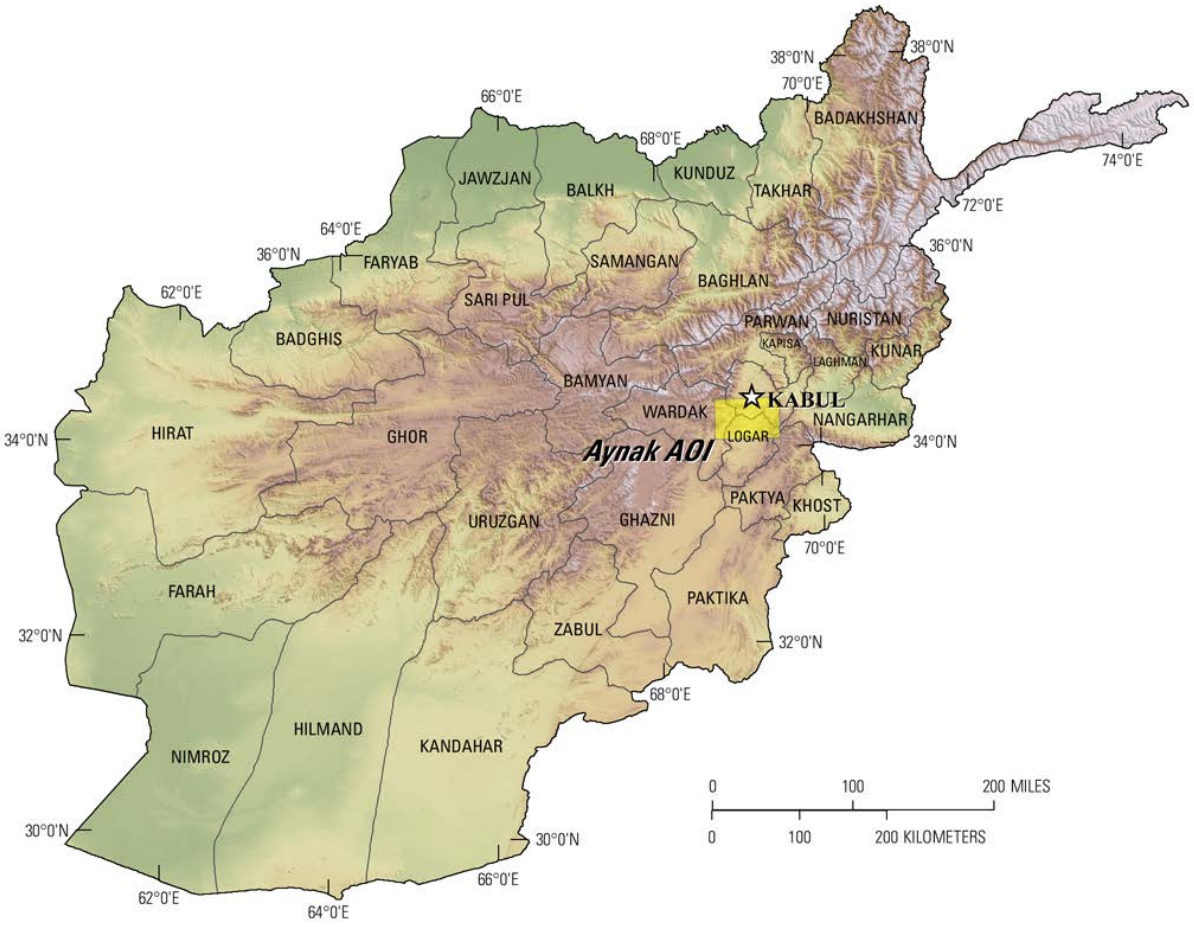

Figure 2B–1. The Aynak–Logar Valley area of interest is located south of Kabul within the Logar, Wardak, and Kabul Provinces of Afghanistan.

2B.1.2 Collection of Imaging Spectrometer Data

The HyMap imaging spectrometer (Cocks and others, 1998) was flown over Afghanistan from August 22 to October 2, 2007 (Kokaly and others, 2008). HyMap has 512 cross-track pixels and covers the wavelength range 0.43 to 2.48 microms (μm) in 128 channels. The imaging spectrometer was flown on a WB-57 high-altitude aircraft at 50,000 feet. There were 207 standard data flight lines and 11 cross-cutting calibration lines collected over Afghanistan for a total of 218 flight lines, covering a surface area of 438,012 square kilometers (Kokaly and others, 2008). Data were received in scaled radiance form (calibrated to National Institute of Standards and Technology reference materials). Before processing, four channels that had low signal-to-noise ratios and (or) were in wavelength regions overlapped by adjacent detectors were removed from the HyMap data (image cubes). Each flight line was georeferenced to Landsat base imagery in Universal Transverse Mercator (UTM) projection (Davis, 2007).

2B.1.3 Calibration Process

HyMap data were converted from radiance to reflectance using a multi-step calibration process. This process removed the influence of the solar irradiance function, atmospheric absorptions, and residual instrument artifacts, resulting in reflectance spectra that have spectral features that arise from

the material composition of the surface. Because of the extreme topographic relief and restricted access to ground calibration sites, modifications to the standard USGS calibration procedures (Clark and others, 2003a) were required to calibrate the 2007 Afghanistan HyMap dataset (Hoefen and others, 2010).

In the first step of the calibration process, the radiance data were converted to apparent surface reflectance using the radiative transfer correction program Atmospheric CORrection Now (ACORN; ImSpec LLC, Palmdale, Calif.). The ACORN program was run multiple times for each flight line, using average elevations in 100-meter (m) increments, covering the range of minimum to maximum elevation within the flight line. A single atmospherically corrected image was assembled from these elevation-incremented ACORN results. This was done by determining the elevation of each HyMap pixel and selecting the atmospherically corrected pixel from the 100-m increment closest to that elevation.

Each assembled atmospherically corrected image was further empirically adjusted using ground-based reflectance measurements from a ground calibration site. Spectra of five ground calibration sites were collected in Afghanistan: field spectra from Kandahar Air Field, Bagram Air Base, and Mazar-e-Sharif Airport, as well as laboratory spectra of soil samples from two fallow fields in Kabul. At each site, the average field spectrum of the ground target was used to calculate an empirical correction factor using the pixels of atmospherically corrected HyMap data in the flight lines that passed over the site. Subsequently, each of the HyMap flight lines was ground-calibrated using the empirical correction from the closest calibration site.

To further improve data quality, an additional calibration step was taken to address atmospheric differences caused, in part, by the large distances between the calibration sites and the survey areas. The large distances were a result of the lack of safe access to ground calibration sites. The duration of the airborne survey and variation in time of day during which flight lines were acquired also resulted in differences in atmospheric conditions between standard flight lines and lines over ground calibration sites, which were used to derive the empirical correction factors. Over the course of the data collection, the sun angle, atmospheric water vapor, and atmospheric scattering differed for each flight line. To compensate for this, cross-cutting calibration flight lines over the ground calibration areas were acquired (Kokaly and others, 2008) and used to refine the reflectance calculation for standard data lines. A multiplier correction for standard data lines, typically oriented as north-south flight lines, was derived using the pixels of overlap with the well-calibrated cross-cutting lines, subject to slope, vegetation cover, and other restrictions on pixel selection (Hoefen and others, 2010). As a result, the localized cross-calibration multiplier, derived from the overlap region, reduced residual atmospheric contamination in the imaging spectrometer data that may have been present after the ground calibration step.

2B.1.4 Materials Maps and Presentation

After undergoing the above calibration process, the georeferenced and calibrated reflectance data were processed. The reflectance spectrum of each pixel of HyMap data was compared to the spectral features of reference entries in a spectral library of minerals, vegetation, water, and other materials (King, Kokaly, and others, 2011; Kokaly and others, 2011). The best spectral matches were determined for each pixel, and the results were clustered into classes of materials discussed below.

HyMap reflectance data were processed using MICA (Material Identification and Characterization Algorithm), a module of the U.S. Geological Survey PRISM (Processing Routines in Interactive Data Language (IDL) for Spectroscopic Measurements) software (Kokaly, 2011). The MICA analysis compared the reflectance spectrum of each pixel of HyMap data to entries in a reference spectral library of minerals, vegetation, water, and other materials. The MICA spectral comparison technique is partly derived from the Tetracorder spectral identification system (Clark and others, 2003b). The HyMap data were compared to 97 reference spectra of well-characterized mineral and material standards. The resulting maps of material distribution, resampled to 23×23 square meter pixel grid, were mosaicked to create thematic maps of surface mineral occurrences over the full dataset covering Afghanistan.

The MICA module was applied to HyMap data twice to present the distribution of two categories of minerals that are naturally separated in the wavelength regions of their primary absorption features. MICA was applied using the subset of minerals with absorption features in (1) the visible and near-infrared wavelength region, producing a 1-µm map of iron-bearing minerals and other materials (King, Kokaly, and others, 2011), and (2) in the shortwave infrared, producing a 2-µm map of carbonates, phyllosilicates, sulfates, altered minerals, and other materials. For clarity of presentation, some individual classes in these two maps were bundled by combining selected mineral types (for example, all montmorillonites or all kaolinites) and representing them with the same color in order to reduce the number of mineral classes.

The iron-bearing minerals map has 28 classes. Iron-bearing minerals with different mineral compositions but similar broad spectral features are difficult to classify as specific mineral species. Thus, generic spectral classes, including several minerals with similar absorption features, such as Fe^{3+} type 1 and Fe^{3+} type 2, are depicted on the map. The carbonates, phyllosilicates, sulfates, and altered minerals map has 32 classes. Minerals with slightly different compositions but similar spectral features are less easily discriminated; therefore, some identified classes consist of several minerals with similar spectra, such as the "chlorite or epidote" class. When comparisons with reference spectra provided no viable match, a designation of "not classified" was assigned to a pixel.

2B.2 Geologic Setting of the Aynak-Logar Valley Area of Interest

The Aynak-Logar Valley AOI is located within northern Logar, eastern Wardak, and southern Kabul Provinces of Afghanistan (fig. 2B–1). The elevation in the AOI ranges from 1,778 to 4,257 m (fig. 2B–2). The Aynak subareas—Kelaghey-Kakhay, Bakhel-Charwaz, Kharuti-Dawrankhel, and Yagh-Darra – Gul-Darra—contain sediment-hosted copper mineralization, whereas the Logar Valley subarea hosts podiform chromite (Peters and others, 2007). The subareas are marked on the elevation map (fig. 2B–2). The contrast-enhanced stretch of the natural-color composite of Landsat Thematic Mapper (TM) bands in figure 2B–3 provides a general overview of the Aynak-Logar Valley AOI terrain and is useful for understanding the general characteristics and distribution of surficial material, including rocks and soil, unconsolidated sediments, vegetation, and hydrologic features.

2B.2.1 Lithology and Structure

Ages of metavolcanic and metasedimentary rocks in the Aynak-Logar Valley AOI are Early to Late Proterozoic; sedimentary rocks in the AOI are Paleozoic, Triassic, Paleocene, Quaternary, and Recent age (fig. 2B–4; Abdullah and Chmyriov, 1977; Doebrich and others, 2006). The Kabul block of accreted terrane underlies most of the AOI and contains most of the mineralized rocks within two sub-regions: the Aynak sediment-hosted copper district on the east, and the Logar Valley podiform chromite ultramafic district in the west-central part of the AOI. The Aynak area contains the metasedimentary folded and faulted Gulkhamid, Loy Khwar, and Welayati Formations, seen within the Vendian complex-Cambrian unit of figure 2B–4. The Logar Valley area contains large bodies of ultramafic rock, seen as the Eocene unit of figure 2B–4, though these rocks are now dated as being pre-Eocene. The far western part of the area, a region of early to middle Proterozoic rock, contains the Paghman metasedimentary and intrusive terrane, which is another highly faulted crustal block containing Proterozoic and Paleozoic rocks (Bohannon, 2010; Volin, 1950).

2B.2.2 Known Mineralization

Figure 2B–5 shows locations where reconnaissance field geology and geologic literature identified mineralization that suggests a potential for mineral resources (Peters and others, 2007; Abdullah and others, 1977). The characteristics of the mineralized locations are summarized in table 2B–1. Although many types of mineralization are indicated, the mineral occurrences in the Aynak-Logar Valley AOI are mainly sediment-hosted copper and podiform chromite. The noted mineral occurrences

listed in table 2B–1 are relatively small and are at or below the spatial resolution of the HyMap data (nominally 23 m).

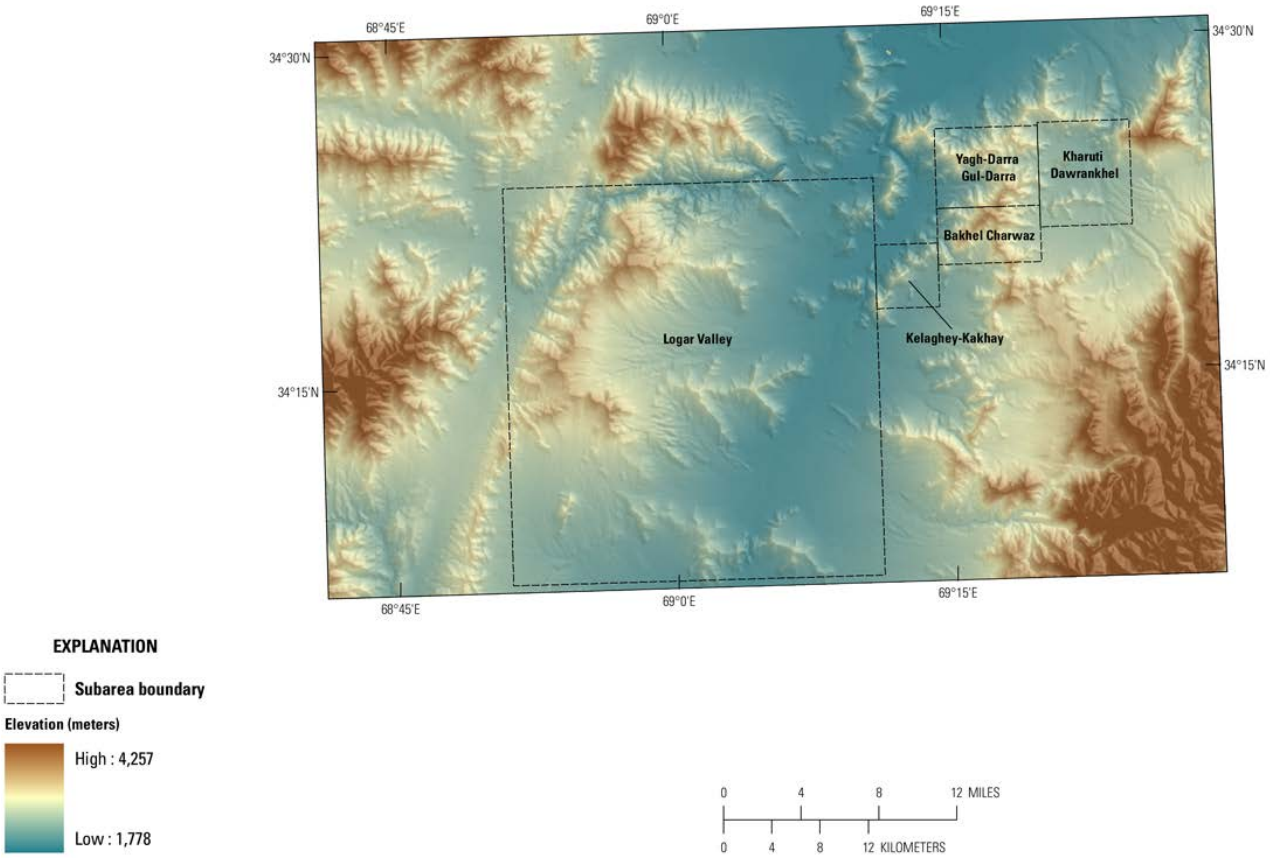

Figure 2B–2. Shaded-relief map showing elevations in the Aynak-Logar Valley area of interest. The darker brown tones indicate higher elevations, and lower elevations are represented by blue tones.

Table 2B–1. Deposit name, deposit type, mineralogy, and alteration of the known sites of mineralization in the Aynak-Logar Valley area of interest.

Deposit name	Polymetallic vein	Silicification	Chalcopyrite	Quartz
Sultan Padshah Stone	Marble	—	No data	No data
Yagh-darra	Sediment-hosted Cu	—	No data	No data
Maydan Stone	Marble	—	No data	No data
Sultan Padshah Copper	Sediment-hosted Cu	Silicification	Chalcopyrite; covellite; malachite;	Quartz
Shanhi-Baranty	Marble	—	No data	No data
Taghar	Sediment-hosted Cu	—	Chalcopyrite; bornite; chalcocite; covellite; malachite; azurite	No data
Unnamed	Sediment-hosted Cu	—	Malachite	No data
Maydan Copper	Polymetallic vein	Silicification; baritization	Malachite;	Quartz; barite
Unnamed	Sediment-hosted Cu	—	No data	No data
Sharar	Marble	—	No data	No data
Khaidarabad Iron	Iron-formation	—	Martite	No data
Khaidarabad Copper	Sediment-hosted Cu	—	Chalcopyrite; malachite	No data

Stratabound copper mineralization is hosted in the Neoproterozoic (Vendian)–Lower Cambrian Loy Khwar Formation. The Loy Khwar Formation copper host rock consists of dolomitic limestone, marl, quartz-biotite-dolomite schist, micaceous carbonate rock, biotite-amphibole schist, and quartzite. Copper mineralization occurs as bornite and chalcopyrite with chalcocite and supergene copper minerals; it is usually hosted in dolomitic marble, limestone, or carbonaceous schists (fig 2B–5). Mineral occurrences trend northeastward through the eastern half of the study area within the Kelaghey-Kakhay, Bakhel-Charwaz, Kharuti-Dawrankhel, and Yagh-Darra–Gul-Darra subareas. The Aynak and associated copper deposits have been extensively explored. The two types of ore, bornite and chalcopyrite, combine for a total known resource of 12,340,000 metric tons (t) of copper. These sediment-hosted copper deposits were most likely formed during lithification as copper-bearing brines were introduced into the Loy Khwar Formation (Peters and others, 2007).

Known copper deposits within the AOI occur mainly within the Aynak subareas. The largest resource, Kelaghey, is estimated to contain 43,000 t of copper at a grade of 0.91 weight percent copper (Peters and others, 2007). Smaller copper occurences trend within two prospective tracts defined by Peters and others (2007). Each tract may represent complex folded layers with mineralization concentrated near the fold crests. An east-trending tract contains the Yagh-darra, Ghuldarra II, and Ghuldarra I prospects (Yagh-Darra–Gul-Darra subarea). In the southwest, a second northeast-trending tract contains the Kelaghey, Sorbog, Katasand, Dashtak, and Kakhay deposits (Kelaghey-Kakhay subarea). Additional deposits in the tract include the Zakhel, Palanghar, Charwazi, and Bagkhei (Barkhei) deposits in the central region (Bakhel-Charwaz subarea), and the Chakari, Kharuti, Mirzakhan, Dawrankhel, and Taghar deposits in the northeast (Kharuti-Dawrankhel subarea) (Peters and others, 2007).

Podiform chromite, along with minor ultramafic-hosted talc, clay, and pegmatite, are found within the Logar Valley (westernmost part) subarea within pre-Eocene ultramafic rocks. The chromite in the Logar Valley subarea occurs within Triassic or Permian massive peridotite that has been suggested as being formed from oceanic lithosphere in the Tethyan ocean (Tapponnier and others, 1981). Eleven sites have been explored through mapping, drilling, trenching, and sampling by Volin (1950), but no consistent structure or orientation was found in the ultramafic rocks. Primary minerals are enstatite and olivine; secondary minerals include chromite, magnetite, and feldspar. Chromite occurs as massive lenses, pods, and irregular bodies, whereas the wall rock was serpentinized then subsequently altered by more recent supergene processes to magnesite and dolomite with red iron oxide (Volin, 1950). Of the eleven sites, sites 1, 2, 3, and 5 (the Logar Deposit) were cored by diamond-drill. Other sites were named Werek, to the north of the Logar Deposit, and Makhmudgazi, to the south. A resource estimate of 181,200 t of ore at 35.8 to 57.5 weight percent Cr_2O_3 was calculated.

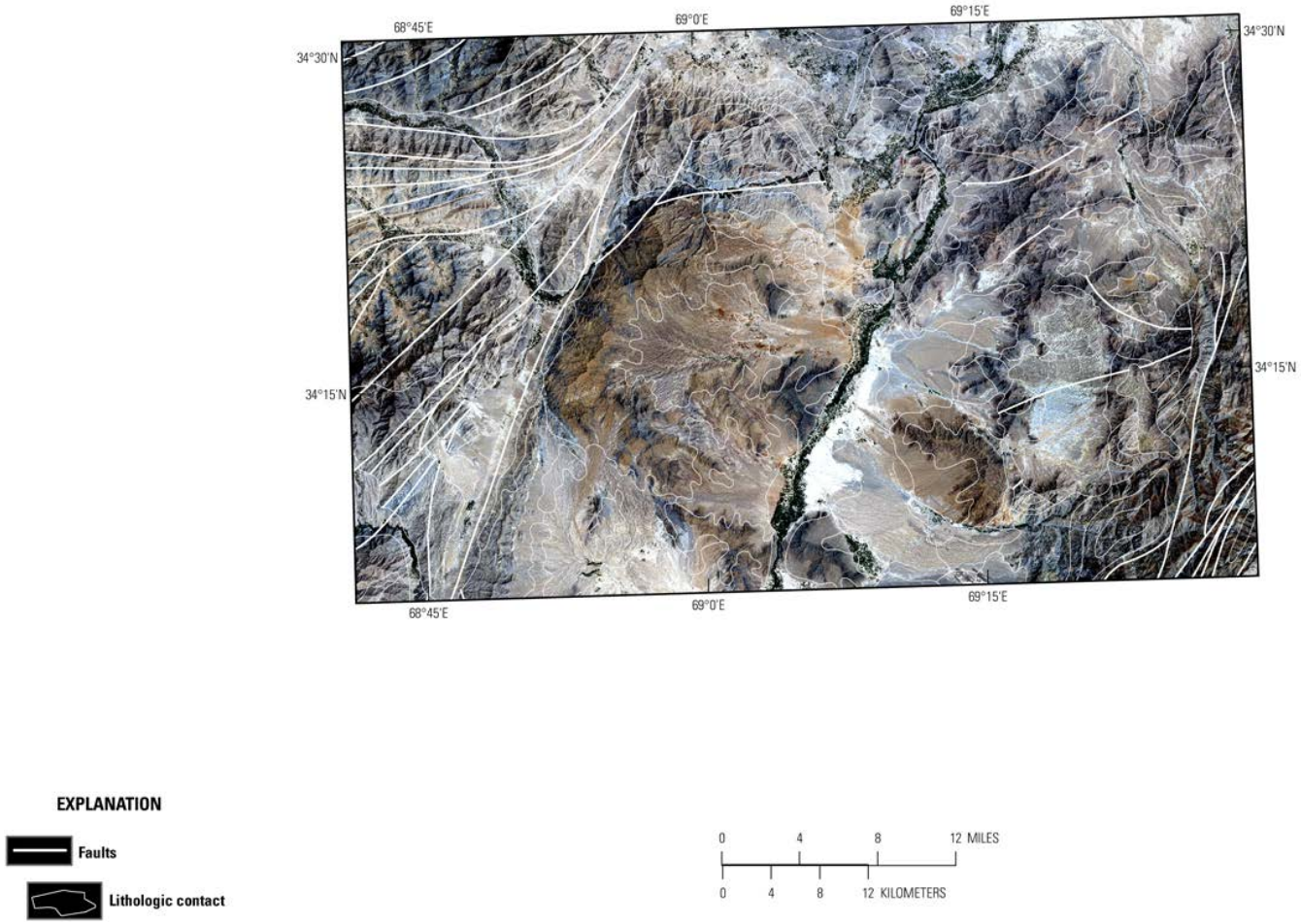

Figure 2B–3. Landsat Thematic Mapper image of the Aynak-Logar Valley area of interest (AOI) (Davis, 2007). Numerous faults and fractures of different orientations and extent occur within the AOI (Doebrich and others, 2006; Abdullah and Chmyriov, 1977).

2B.3 Mineral Maps of the Aynak-Logar Valley Area of Interest

Analysis of the HyMap data of the Aynak-Logar Valley AOI using spectroscopic methods (Kokaly, 2011) resulted in the detection and mapping of the distributions of a variety of surficial minerals. Reflectance spectra of well-characterized reference minerals and other materials were compared to the spectrum of each HyMap pixel. The best match between each pixel and the materials in the reference library were identified based on the wavelength position and shapes of absorption features in the 0.45–2.48 μm wavelength region. The results were divided into two general categories of minerals: (1) iron-bearing minerals that have characteristic spectral absorption features that occur at wavelengths in the visible to near-infrared wavelength region, and (2) a wide variety of minerals, including carbonates, mica and clay minerals, and sulfates, that have diagnostic spectral absorptions in the 2-μm region. Although the occurrence of certain minerals may suggest mineralization processes may have occurred in the area, many of the minerals identified and mapped are also common rock-forming minerals or minerals that can be derived from the weathering of a variety of rock types. Consequently, the distribution patterns of the identified minerals and the geologic content where they occur are extremely important in understanding the causes of the mapped mineral occurrences and assessing the possible potential for related mineral deposits.

The maps of surface materials are presented in several ways: (1) maps showing the entire suite of minerals in the 2-μm and 1-μm categories, figures 2B–6 and 7, respectively, and (2) thematic maps that are subsets of the reference materials. The thematic maps, which depict selected groups of minerals that

are mineralogically related or commonly occur together, are presented to show subtleties in the mineral distribution (figs. 2B–8 to 2B–12). Figure 2B–8 shows the distribution of carbonate minerals in the AOI, whereas figure 2B–9 shows where the clays and micas were mapped. The distribution of iron-oxide and iron-hydroxide minerals are displayed in figure 2B–10. Secondary minerals are shown in figure 2B–11, and minerals commonly found in hydrothermally altered rocks are mapped in figure 2B–12. HyMap data are also a powerful tool to use in the identification and mapping of faults and fractures (see fig. 2B–9); note the correlation between mapped minerals and fault traces. Following the presentation and discussion of the maps of the full Aynak-Logar Valley AOI, detailed maps of the subareas are presented. A companion report and geodatabase of potential mineral resource anomalies (areas of a potential economic mineral resource occurrence), which have not been previously known or where the HyMap data has expanded the knowledge or surficial coverage, can be found in King, Johnson, and others (2011).

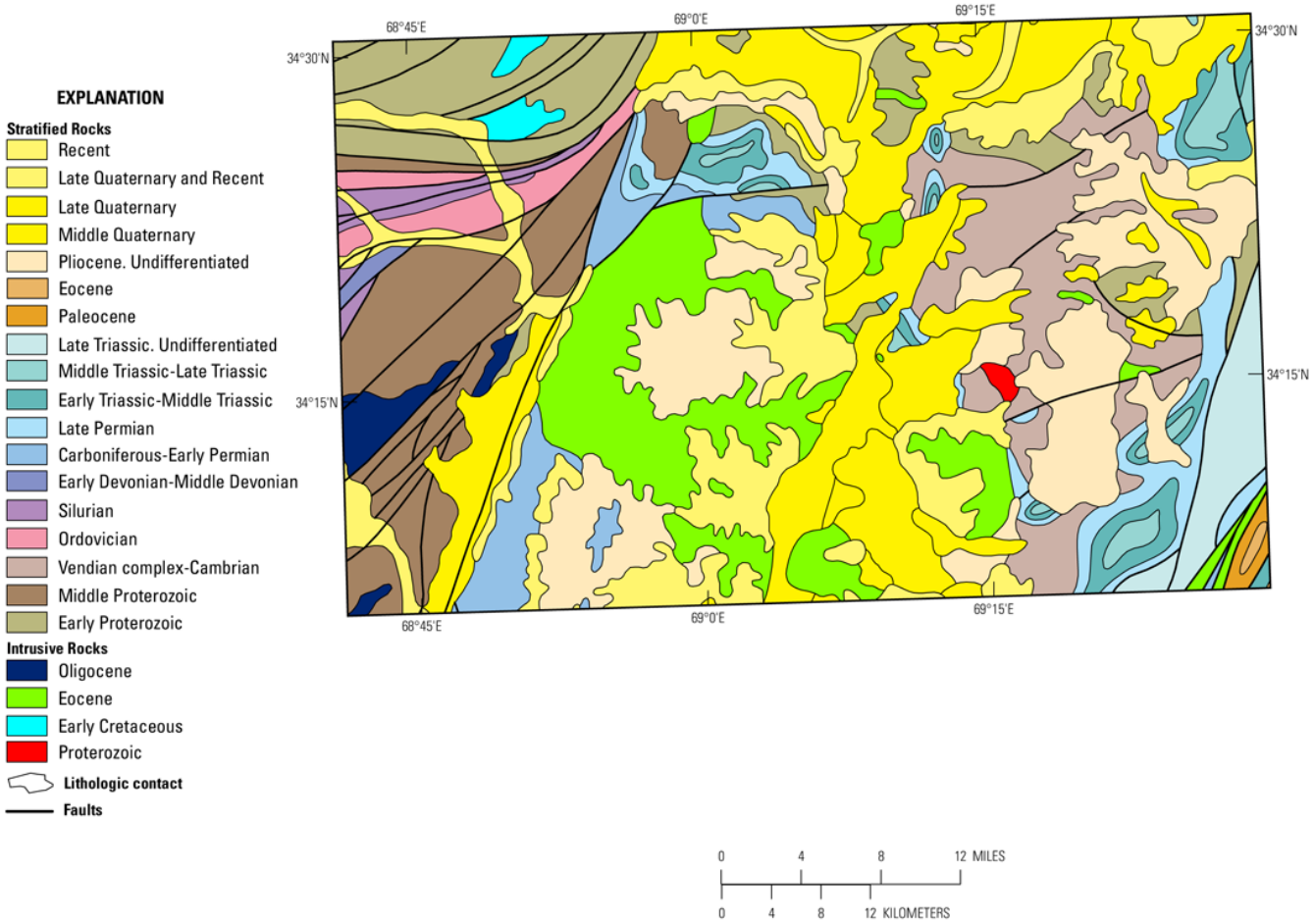

Figure 2B–4. Geologic map of the Aynak-Logar Valley area of interest taken from Doebrich and others (2006) and Abdullah and Chymriov (1977).

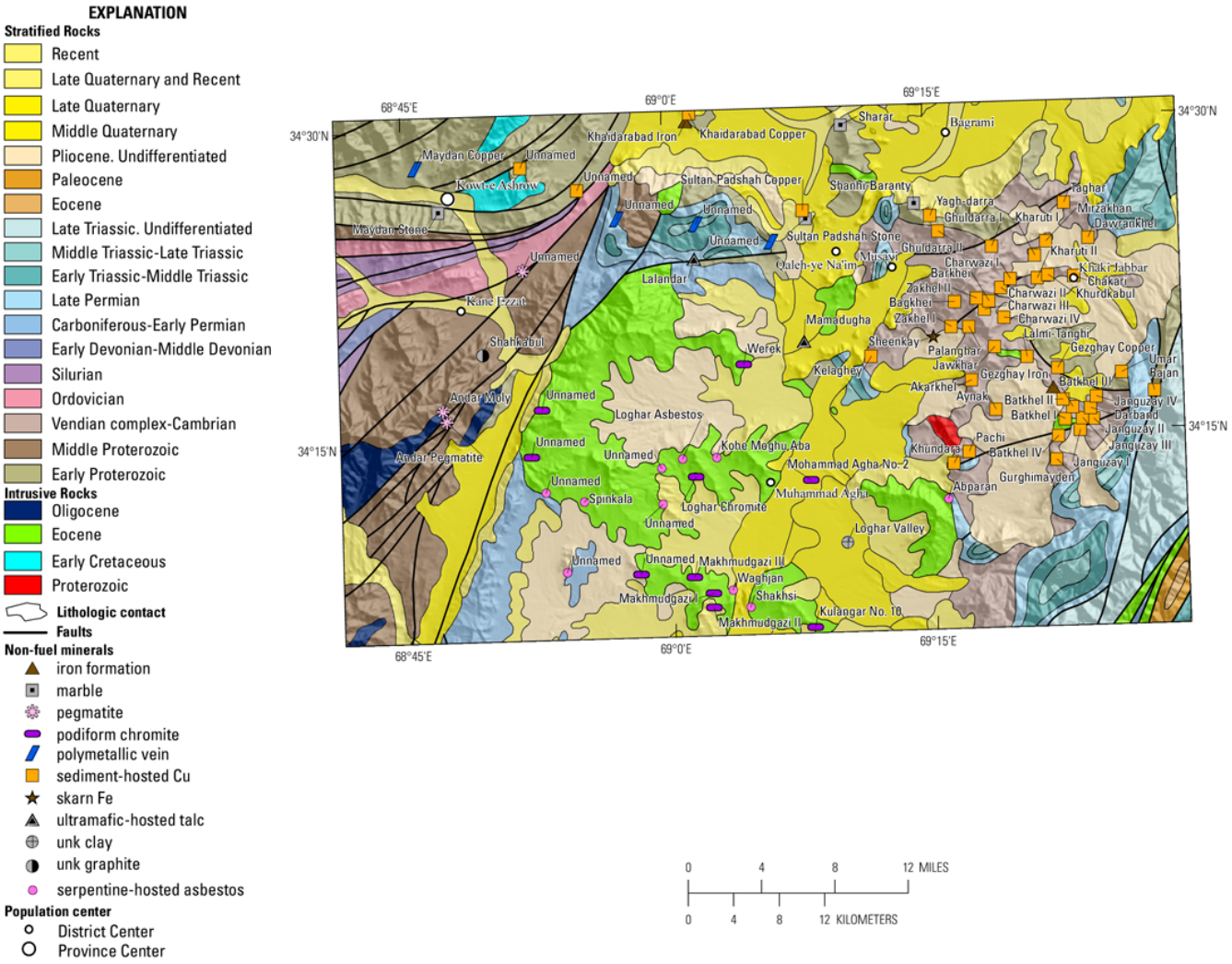

Figure 2B–5. Location of known mineral occurrences in the Aynak-Logar Valley area of interest. The map consists of four data layers: shaded-relief base map; transparency of the geologic map (Dronov and others, 1972), fault traces (Peters and others, 2007), and known mineral occurrences (Peters and others, 2007). Unk, unknown.

2B.3.1 Aynak-Logar Valley Area of Interest

Figures 2B–6 and 2B–7 show the distribution of carbonates, phyllosilicates, sulfates, altered minerals, and other materials (2-µm map) and the Fe-bearing minerals (1-µm map) for the entire Aynak-Logar Valley AOI. The Aynak-Logar Valley AOI contains a variety of lithologies and structural trends, hosting a diverse range of mineralization.

The two crustal plates and their suture zone show distinct mineral distribution patterns. Paghman metasedimentary rocks on the west show highly contorted alignments of mica-rich units, with calcite and chlorite-bearing units that have undergone severe deformation. The central area (Kabul block), contains large masses of serpentine-rich ultramafic rock with chlorite and (or) epidote-bearing contact zones. Paleozoic carbonate rocks surround the ultramafics on the north and south. To the east, carbonate-bearing metasedimentary layered rock is exposed. Alluvium cover contains abundant mica and clay. Importantly, a sense of structure is seen in the warping of a narrow Paleozoic dolomite unit twisting southward along the eastern boundary. Iron-bearing minerals reflect the importance of mafic rock compositions in the eastern region (as well as the central ultramafic area), where outcropping formations again define regional structure.

Generally, the eastern region is carbonate rich within the Gulkhamid, Loy Khwar, and Welayati Formations (Vendian complex-Cambrian unit in fig. 4; see Bohannon, 2010 for details of the units), as

well as in areas with other Paleozoic rocks (fig. 2B–8). The western portion of the Logar Valley region contains large tracks of serpentine and iron-bearing ultramafic rocks with Proterozoic rocks to the west containing muscovite.

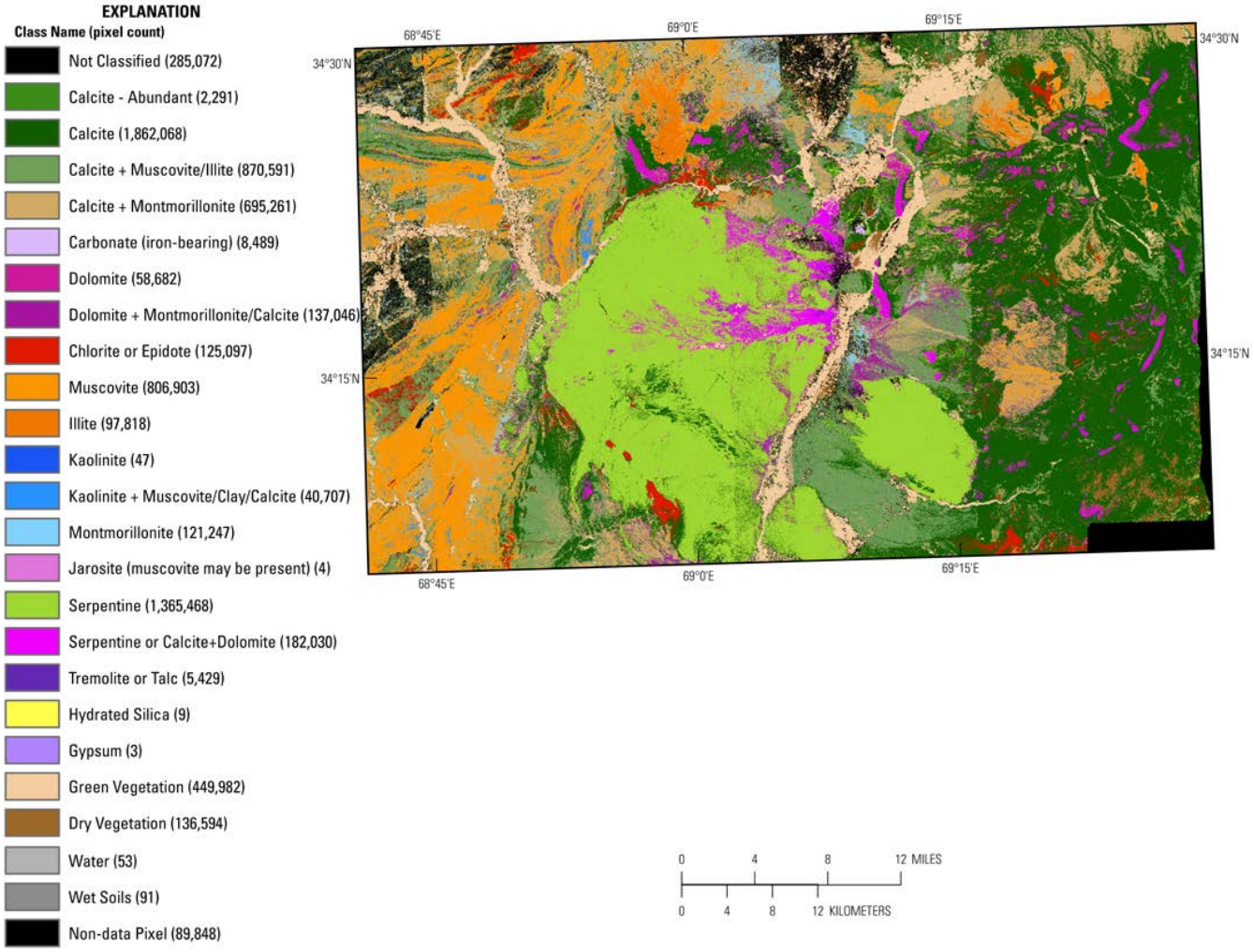

Figure 2B–6. Distribution of clays, carbonates, phyllosilicates, sulfates, altered minerals, and other materials detected in the HyMap data for the Aynak-Logar Valley area of interest.

2B.3.1.1 Carbonate Minerals

Mapped minerals correlate well with lithology within these subareas. Although spectral mapping did not detect individual ore minerals or deposit-related altered minerals, it did detect permissive host rock areas, especially areas containing dolomitic marble country rock. Geologic structures within the copper-bearing host rock Loy Khwar Formation trend southwest-northeast in the central part of the subareas and contain erosionally resistant outcrops with bluish-purple shades with light pink-brown lenses in the Landsat TM data (Davis, 2007) (fig. 2B–3). On the spectral mineral maps, these pink-brown lenses have abundant dolomite plus calcite, but were field-mapped by Bohannon (2010) as plagiogranite and syenite porphyries. The apparent relation is unclear. They occur mainly within these eastern subareas and may help define the northern extent of the Loy Khwar Formation. Alluvium covers the lower slopes.

The Paghman area on the far west clearly shows lithologies bearing calcite, calcite with mica, and calcite with clay within faulted terrane. The central region shows calcite in contact (north and south) with ultramafic rock. Abundant calcite-bearing bedrock and calcite with mica-bearing alluvium occur throughout the eastern region.

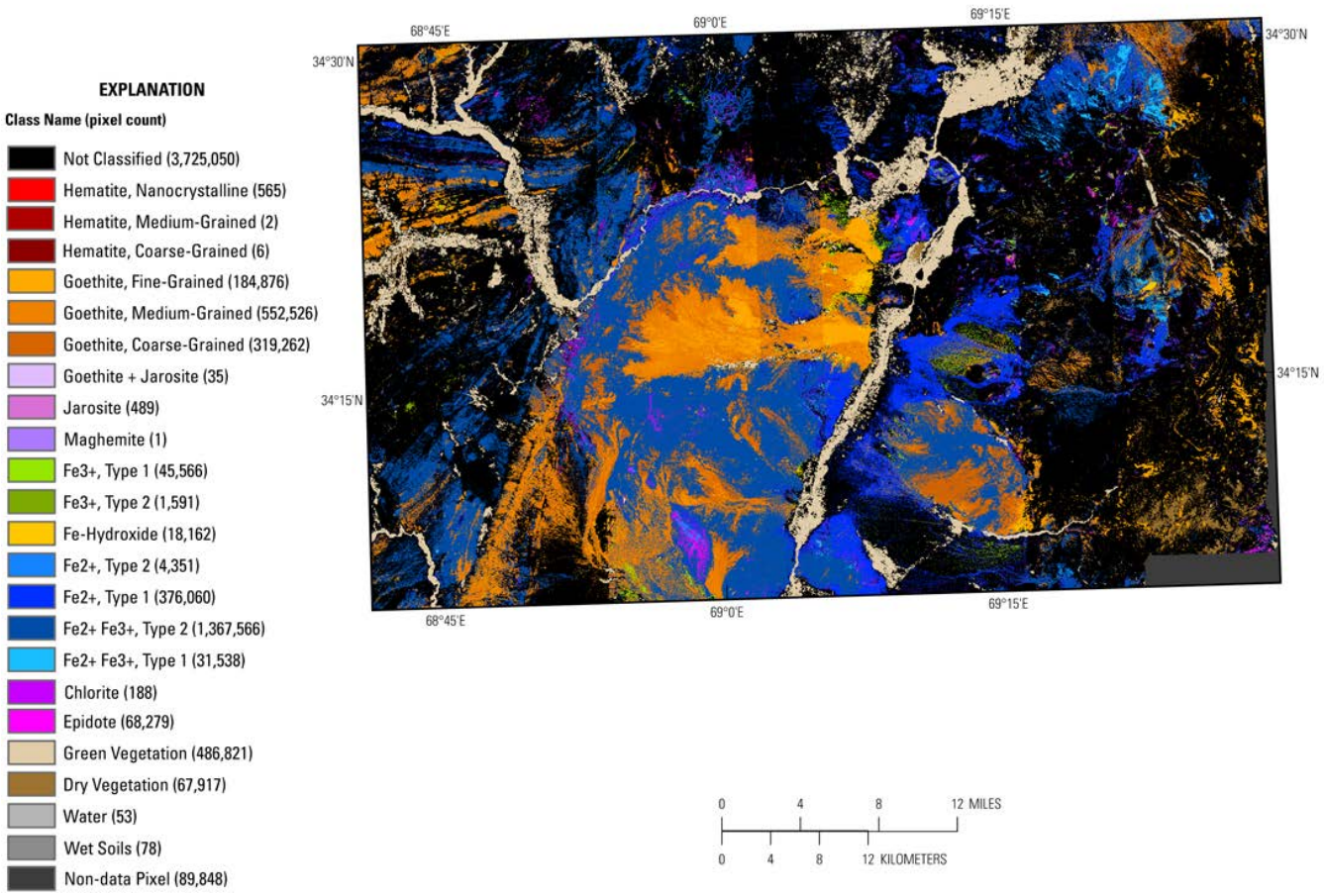

Figure 2B–7. Iron-bearing minerals and other materials in the Aynak-Logar Valley area of interest that were detected in the HyMap data.

2B.3.1.2 Clays and Micas

Clays and mica occur within the alluvial cover but are not identified over much of the area because of spectrally dominant calcite and serpentine spectral signatures (fig. 2B–9). Abundant mica is seen within Proterozoic rock on the western side of the AOI (Paghman area), along with chlorite and (or) epidote apparently following bedding or structural planes.

2B.3.1.3 Iron Oxides and Iron Hydroxides

Figure 2B–10 shows the Fe-bearing minerals in the Aynak-Logar Valley AOI. These Fe-bearing minerals occur primarily in three areas. Ferric and ferrous iron-bearing minerals with goethite are abundant within the Logar Valley ultramafic complex. These minerals are also abundant north of the copper district and west in the Paghman area within Proterozoic rock, again apparently following bedding or structural planes.

2B.3.1.4 Common Secondary Minerals

The occurrence and distribution of secondary minerals for the AOI are shown in figure 2B–11. This map shows information taken from both the 1-µm and 2-µm mineral mapping categories. The Logar Valley ultramafic rock contains abundant serpentine and chlorite and (or) epidote, whereas sparse occurrences of calcite mixed with dolomite and chlorite and (or) epidote correlate with various igneous or metamorphic rocks described in more detail in the Aynak subareas section.

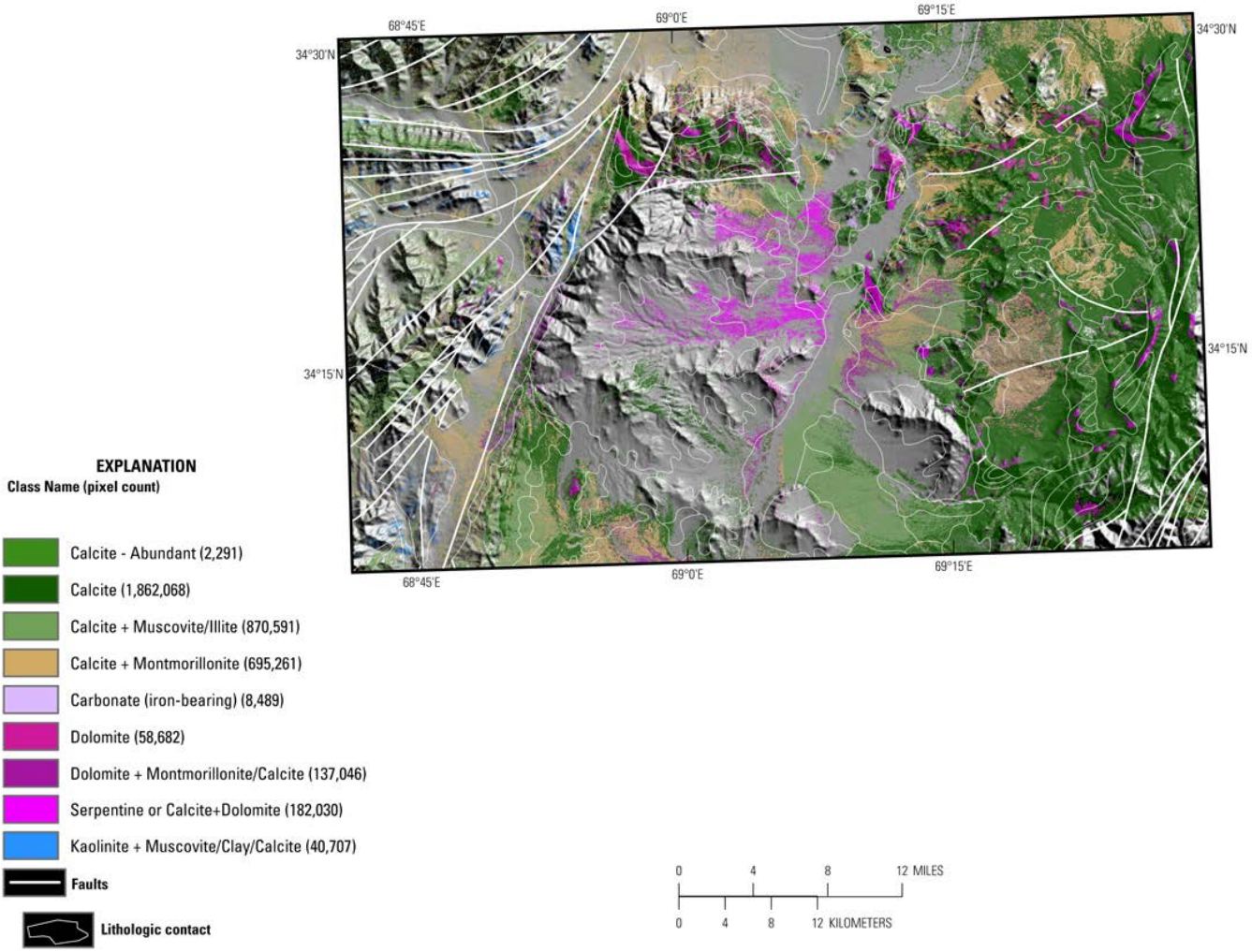

Figure 2B–8. Distribution of carbonate-bearing minerals detected by the HyMap data in the Aynak-Logar Valley area of interest.

2B.3.1.5 Common Alteration Minerals

Most of the minerals in this group (fig. 2B–12) are commonly present in hydrothermally altered rocks associated with epithermal alteration processes. Consequently, where they occur in distinct pixel clusters is of great interest in terms of their association with potential mineral deposits. Altered minerals are sparce, except along the Logar Valley ultramafic contact with other Paleozoic and Proterozoic rocks where chlorite or epidote occur. Chlorite and kaolinite were noted within Proterozoic rock west of the chromite region and are also associated with amphiboles on the eastern side of the AOI.

2B.3.2 Aynak Subareas (Kelaghey-Kakhay, Bakhel-Charwaz, Yagh-Darra–Gul-Darra, and Kharuti-Dawrankhel)

The known mineral occurrence maps (semitransparent geologic maps overlain on shaded-relief images) show the positions of reported mineral occurrences (only sediment-hosted copper) in the Aynak subareas (fig. 2B–13). The topography in the area ranges from 1,818 to 2,935 m, with three subareas encompassing mineralized exposures that trend along southwest-northeast topographic ridges (Kelaghey-Kakhay, Barkheo-Charwaz, and Kharuti-Dawrankhel) and along a southeast-northwest ridge within the Yagh-Darra–Gul-Darra subarea. (fig. 2B–14). Descriptions for these four eastern subareas are grouped together in this section to describe the mineralized district as a whole.

The geologic map of the area (fig. 2B–15) shows nonintrusive rocks with ages of Proterozoic, Cambrian, Late Permian, Pliocene, and Quaternary. The Welayati (Neoproterozoic), Loy Khwar (Neoproterozoic or Cambrian), and Gulkhamid (Cambrian) Formations of metamorphosed sedimentary and igneous rocks cover this area extensively (shown as the Vendian complex-Cambrian unit within fig. 2B–5). Figure 2B–16 displays closeups of the previously mentioned copper mineralization host rocks, and the light pink-brown lenses that are associated with dolomite minerals at this location.

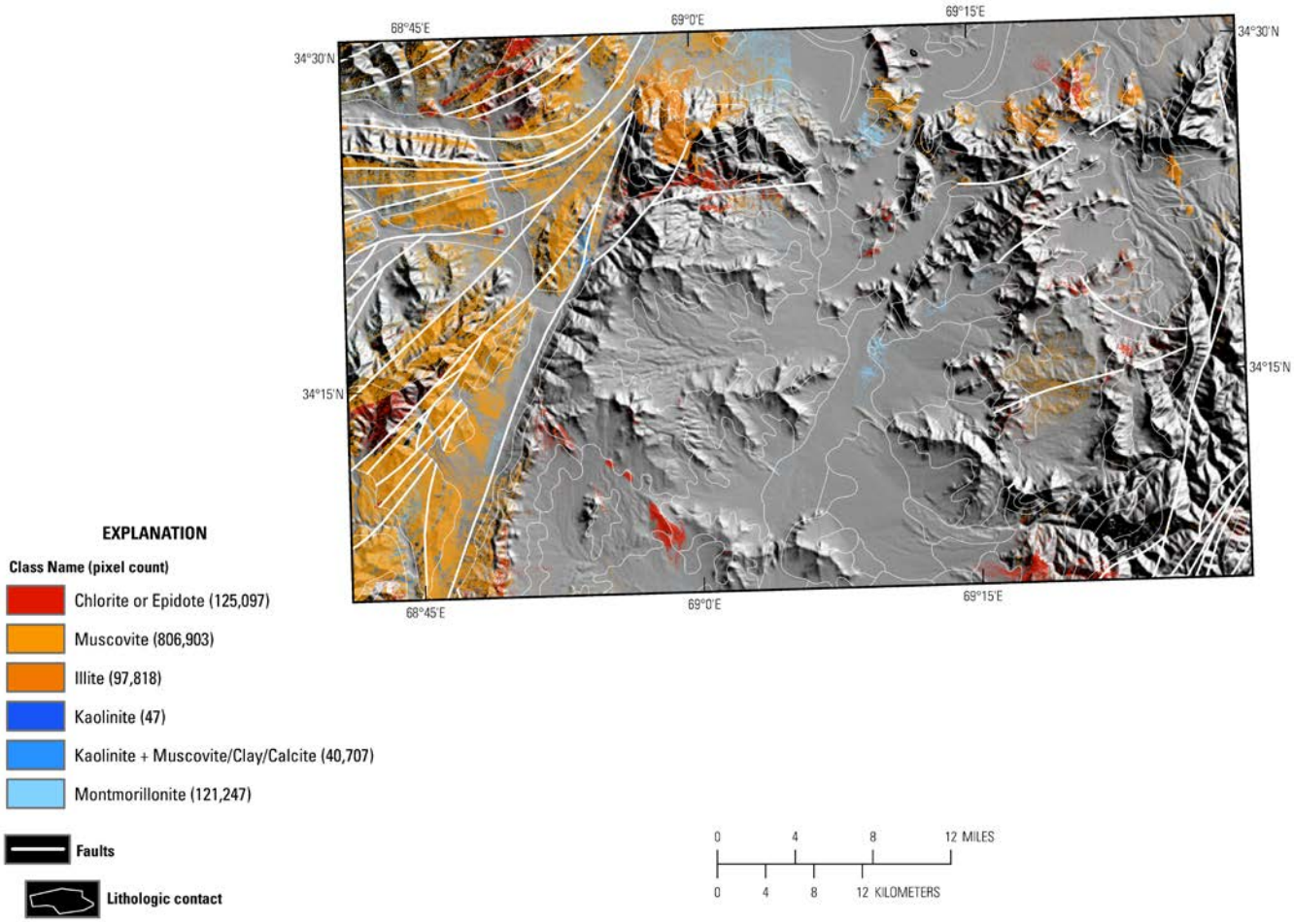

Figure 2B–9. Distribution of clays and micas identified in the HyMap data for the Aynak-Logar Valley area of interest.

Figures 2B–17 and 2B–18 show the distribution of Fe-bearing and carbonate/clay-bearing minerals, respectively. The map of Fe-bearing minerals (fig. 2B–17) displays their lack of abundance within the metasedimentary rock, but their abundance (green and yellow) in association with chlorite and (or) epidote (magenta) within amphibole-bearing masses of the Welayati Formation, stratigraphically below the Low Khwar. Goethite generally maps within alluvium. The map of carbonate/clay-bearing minerals (fig. 2B–18) shows extensive calcite (green) within the subareas and extends outside of them to the north, east, and south. The region is dominated by calcite-rich bedrock. What mapped as dolomite + calcite (colored magenta and should not be confused with the Paleozoic carbonates to the east, outside the subareas) is highly associated with a Cambrian intrusive lens of plagiogranite and syenite and may be a spectral marker for the Welayati-Low Khwar-Gulkhamid complex of rocks. The northeast trend of these intrusive rocks follows the trend of copper mineralization. Chlorite and (or) epidote (red) is associated with amphibolite in the subareas, whereas older gneisses on the northern boundary have abundant muscovite (orange), and alluvium contains calcite with clay (pale brown).

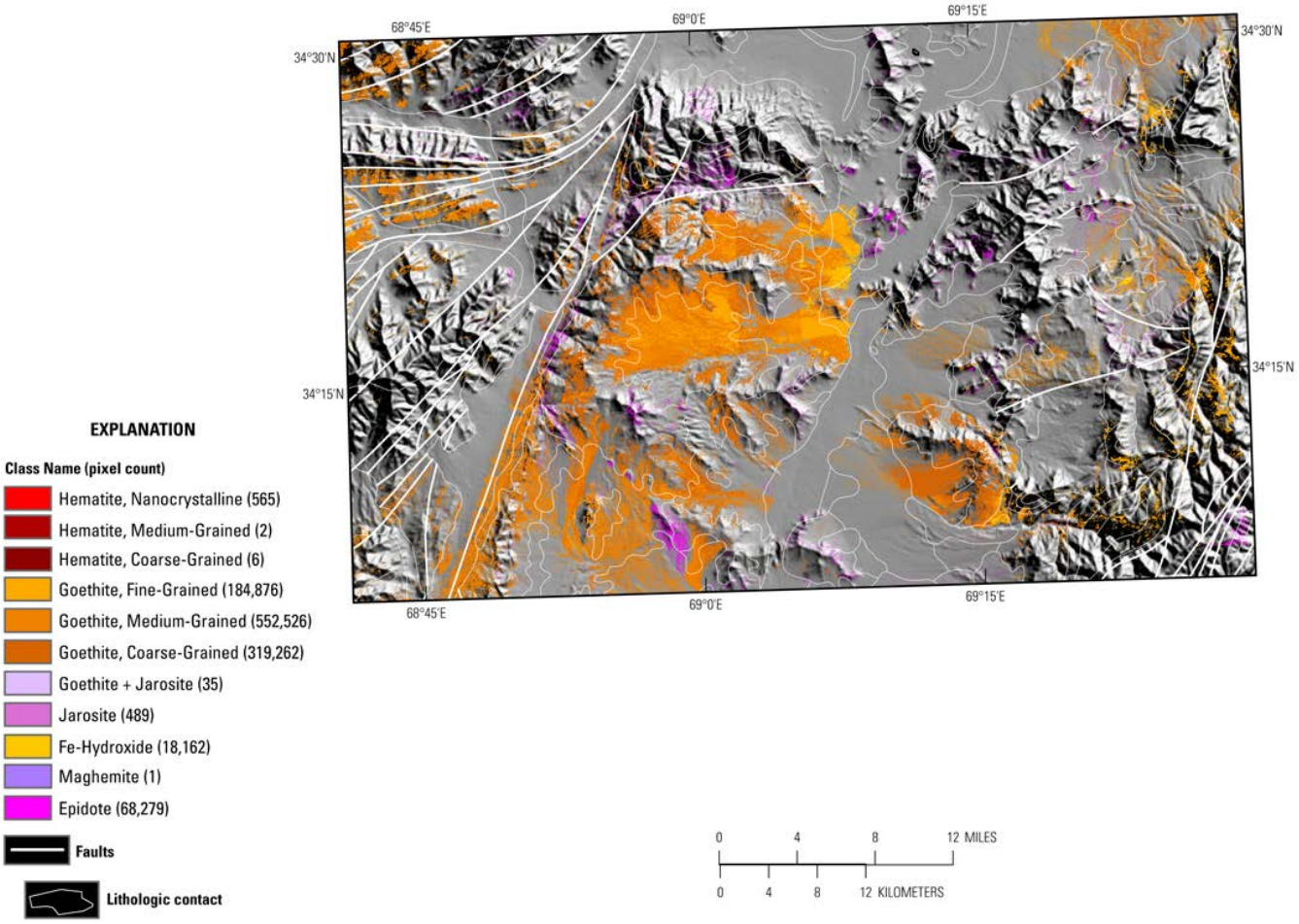

Figure 2B–10. Distribution of iron hydroxides and iron oxides mapped using the HyMap data for the Aynak-Logar Valley area of interest.

2B.3.2.1 Aynak Subareas: Carbonate Minerals

Calcite-rich rocks (green within map) are widespread throughout the subareas but are not diagnostic solely for the copper-bearing lithologies (fig. 2B–19). Dolomite- and calcite-bearing rock (magenta) within the Welayati-Low Khwar-Gulkhamid complex of rocks is associated with lenses of Cambrian igneous rocks, though their apparent relation is unclear. Both trend with the copper mineralization.

2B.3.2.2 Aynak Subareas: Clays and Micas

Within figure 2B–20, mapped clays and micas occur on the northern boundary of the Yagh-Darra–Gul-Darra subarea but are not diagnostic for spectrally locating copper mineralization or host rock. Abundant mapped carbonate overwhelm these spectral signatures.

2B.3.2.3 Aynak Subareas: Iron-Oxide and Iron-Hydroxide Minerals

Figure 2B–21 shows the distribution of iron-oxides and iron-hydroxides in the Aynak subareas. Chlorite and (or) epidote (magenta) are generally associated with amphibole-bearing masses of the Welayati Formation, stratigraphically below the Low Khwar. Chlorite and goethite (light brown) map within alluvium.

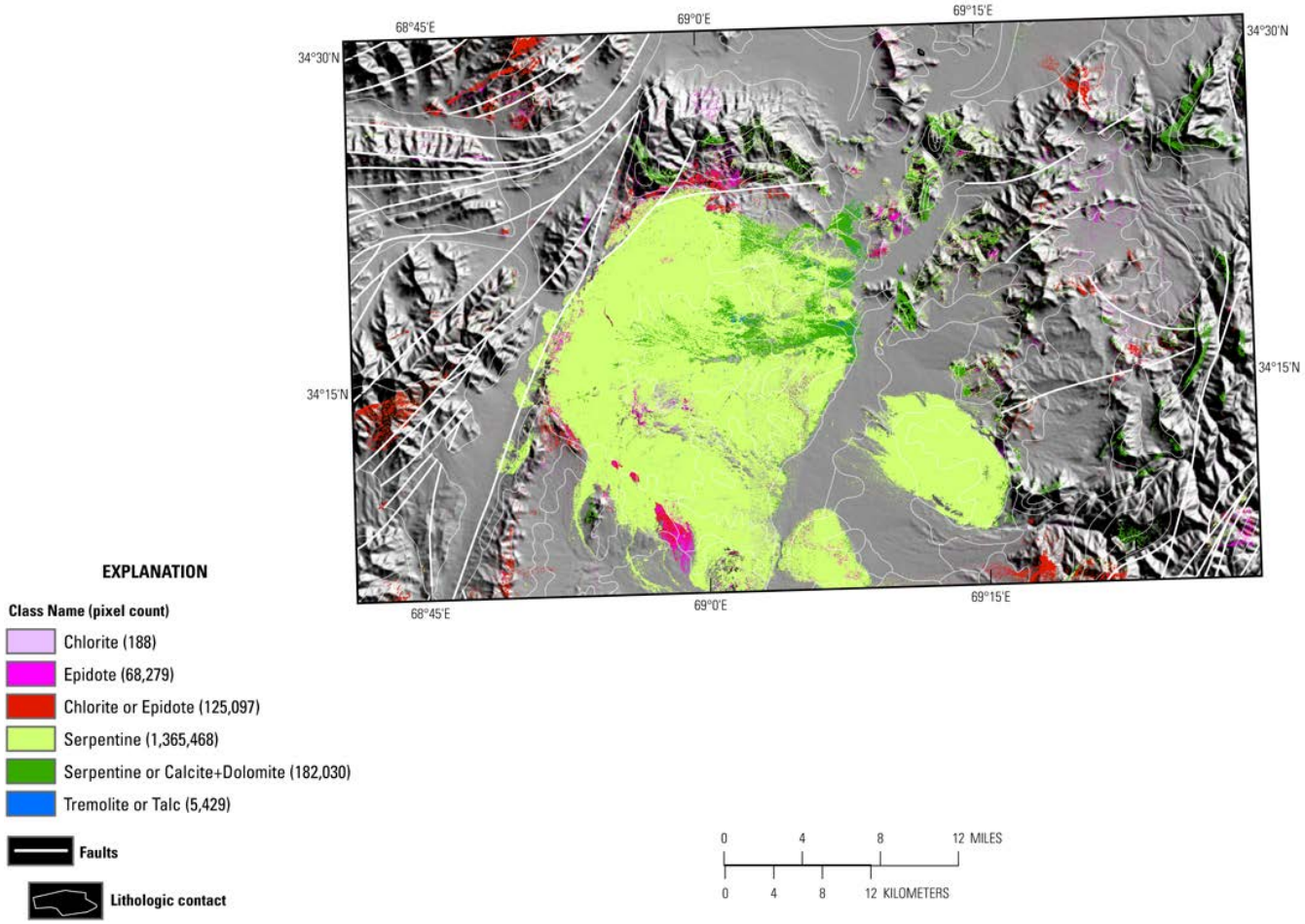

Figure 2B–11. Occurrence and distribution of common secondary minerals detected in the HyMap data for the Aynak-Logar Valley area of interest.

2B.3.2.4 Aynak Subareas: Common Secondary Minerals

There is a scattered distribution of common secondary minerals (fig. 2B–22) in the area. Dolomite with calcite is mapped dark green in this image, without the "spectrally pure" dolomite included in the previous maps. The intrusive rock correlates with this mineral class, but the correlation greatly increases when the dolomite class is included. Epidote and chlorite classes are included as magenta (iron maps) and red (carbonate/clay/mica maps).

2B.3.2.5 Common Alteration Minerals

Most of the minerals in this group (fig. 2B–23) are commonly present in hydrothermally altered rocks associated with epithermal processes. Consequently, where they occur in distinct pixel clusters is of great interest in terms of their potential to help locate possible mineral deposits. Altered minerals within the Aynak subareas are sparce, except for minor chlorite and (or) epidote, especially within the Yagh-Darra–Gul-Darra subarea (top center box, fig. 2B–23), where small clusters occur along what are possibly topographic structural trends.

2B.3.3 Logar Valley Subarea

The known mineral occurrence map (semi-transparent geologic map overlain on a shaded-relief image) shows the approximate positions of reported mineral occurrences in the Logar Valley subarea (fig. 2B–24). Podiform chromite dominates the known mineralization, with ultramafic-hosted talc, clay, and pegmatite (Proterozoic rock) in lesser amounts. The topography in the area ranges from 1,809 to

3,003 m (fig. 2B–25). Ultramafic rock, labeled as Eocene intrusive on the geologic map (Abdullah and Chmyriov, 1977; fig. 2B–26), has now been dated as Triassic or Permian by Tapponnier and others (1981).

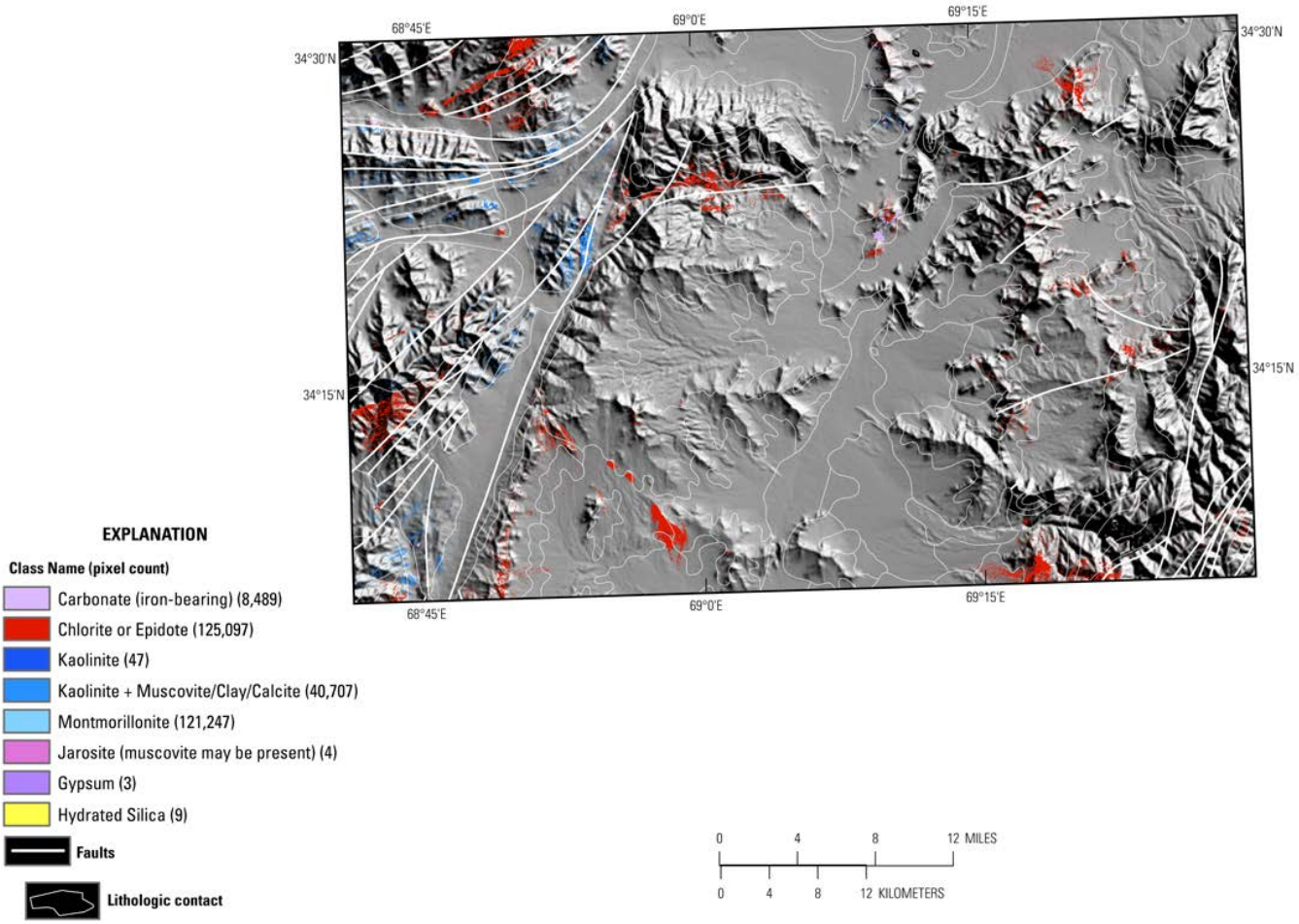

Figure 2B–12. Distribution of common alteration minerals in the Aynak-Logar Valley area of interest.

In the Landsat TM data (fig. 2B–27; Davis, 2007), ultramafic rocks occur within areas of moderate topographic relief and can usually be traced by their brown to dark grayish-blue color. Alluvial fans derived from ultramafic sediments are gently sloping, lighter colored areas within the interior boundary of the ultramafic rock.

The hyperspectral data for the area (figs. 2B–28 and 2B–29) show the distribution of Fe-bearing and carbonate, phyllosilicate, sulfate, alteration minerals, and other materials, respectively. Serpentine, with ferrous- and ferric-iron minerals, was mapped in areas underlain by ultramafic wall rock associated with chromite mineralization. Within interior alluvial fans, the ultramafic sediments contain abundant serpentine and (or) a mix of calcite and dolomite along with goethite. Talc, clay, and pegmatite resources also occur in this subarea. Ultramafic-hosted talc is found near alluvial fan material containing serpentine or a mix of calcite and dolomite, with goethite. Pegmatite is found within Proterozoic rocks lacking strong spectral signatures.

2B.3.3.1 Logar Valley Subarea: Carbonate Minerals

Figure 2B–30 displays widespread distribution of minor carbonate- and clay-carbonate-rich rocks over the entire subarea. A northwest- to southeast-trending band of calcite (green) within the serpentine crops out just south of the largest chromite deposits (labeled Cr) within this subarea described by Volin (1950). Also, very fine detailed linear features of calcite appear within this band. The

implications of this calcite occurrence are unknown, but serpentine is known to alter in this area to dolomite (Volin, 1950).

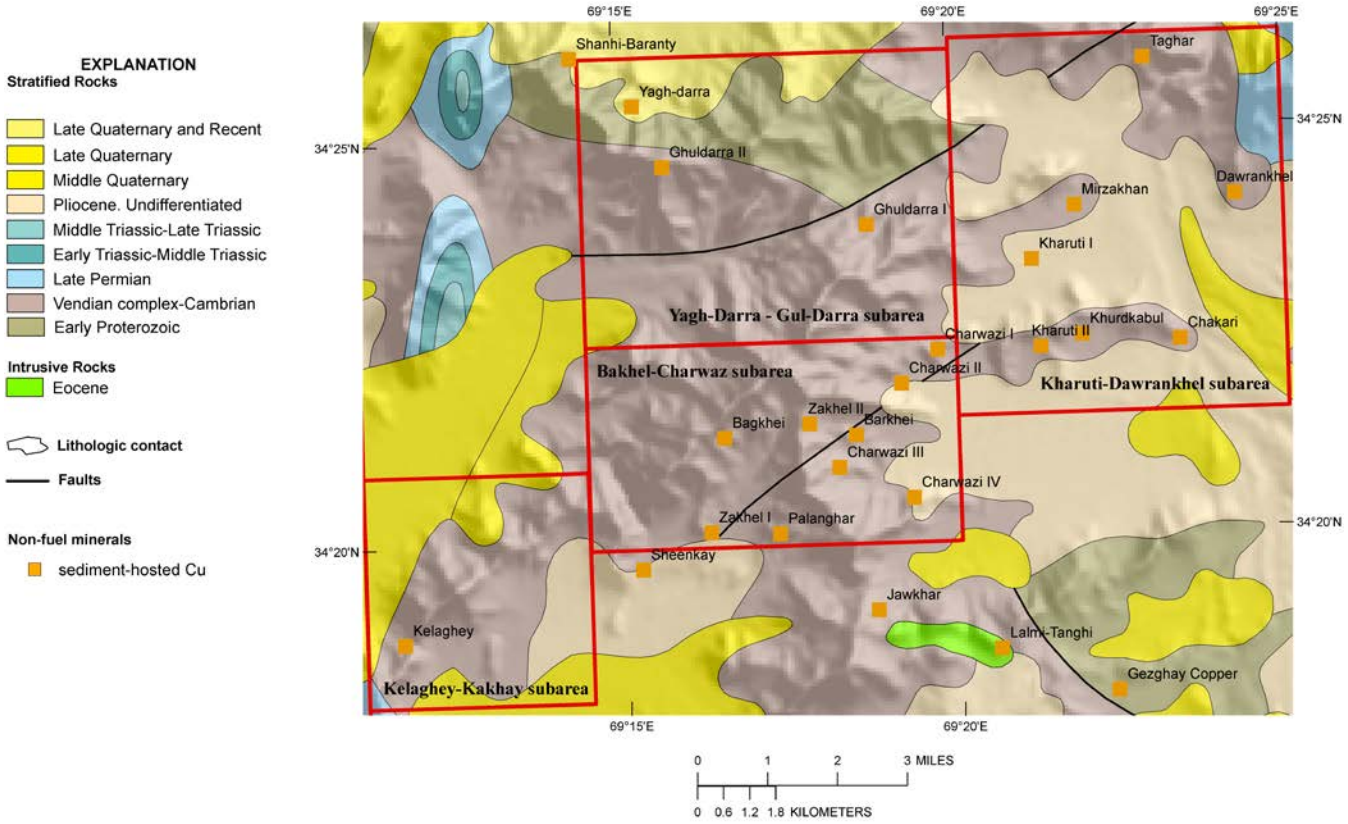

Figure 2B–13. Known mineral occurrences in the Aynak subareas of the Aynak-Logar Valley area of interest: Kelaghey-Kakhay, Bakhel-Charwaz, Yagh-Darra–Gul-Darra, and Kharuti-Dawrankhel.

An abundant zone of serpentine or calcite + dolomite (spectrally, we cannot distinguish between the two groups) trends west to east through most of the image and is correlated with a large eastward-flowing alluvial fan. The presence of abundant dolomite in the alluvial fan shows the abundant character of the ultramafic parent rock within this region, contrasted with the calcite-rich westward flowing fans to the east.

2B.3.3.2 Logar Valley Subarea: Clays and Micas

Figure 2B–31 shows the enrichment of phyllosilicates in the Logar Valley subarea. Chlorite and (or) epidote is identified along the ultramafic rock contact with Paleozoic limestones on the north and south edges of the subarea. Clay, on the east side of the subarea, occurs at the contact of an ultramafic-rock-derived fan with an alluvial fan. Additional clay, surrounded by muscovite, is seen within the Paghman metasedimentary rocks in the northwest corner of the subarea.

2B.3.3.3 Logar Valley Subarea: Iron Oxides and Iron Hydroxides

Iron hydroxides in the subarea are shown in figure 2B–32. Goethite dominates the AOI, especially within alluvial fan areas, and likely indicates oxidation of iron minerals in bedrock of the region. The two abundant goethite-bearing alluvial fans in the north half of the subarea are derived from ultramafic rock. Chlorite and (or) epidote occur along the ultramafic rock contact.

2B.3.3.4 Logar Valley Subarea: Common Secondary Minerals

There are abundant occurrences of the common secondary minerals serpentine, chlorite and (or) epidote, and possibly calcite with dolomite (fig. 2B–33) within the subarea. Serpentine is associated with the ultramafic rock, whereas chlorite and (or) epidote occurs along the boundaries of the ultramafic rock contact. Possible calcite with dolomite (or serpentine) occurs within the ultramafic-sediment-derived alluvial fan.

2B.3.3.5 Logar Valley Subarea: Common Alteration Minerals

The only significant common alteration minerals mapped are the previously mentioned chlorite and (or) epidote groups (fig. 2B–34) that occur along the ultramafic rock contact. Clays occur to the northeast within Middle Proterozoic rock.

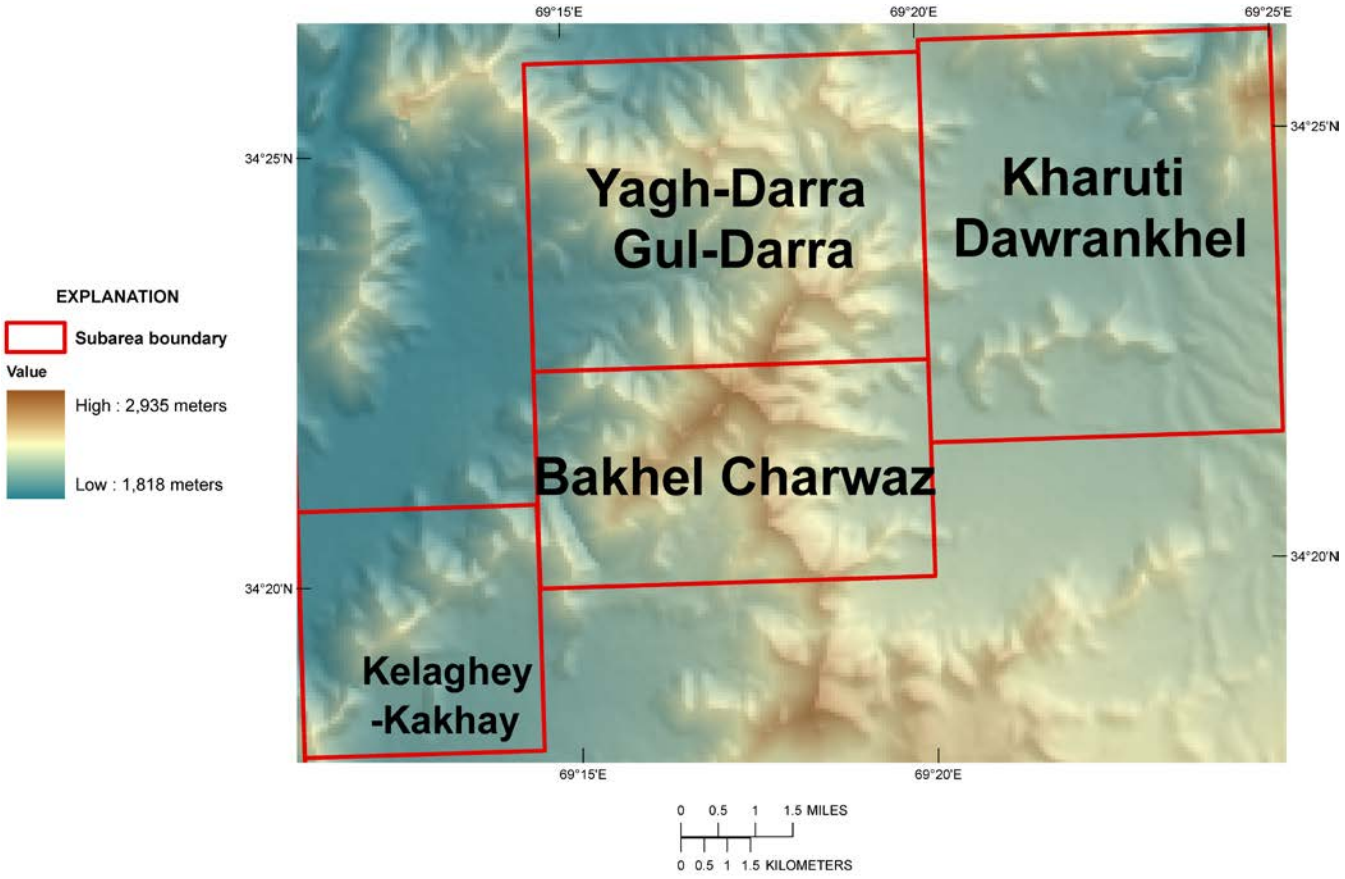

Figure 2B–14. Shaded-relief map showing elevations in the Aynak subareas of the Aynak-Logar Valley area of interest. Darker brown tones indicate the higher elevations, and the lower elevations are represented by the blue tones.

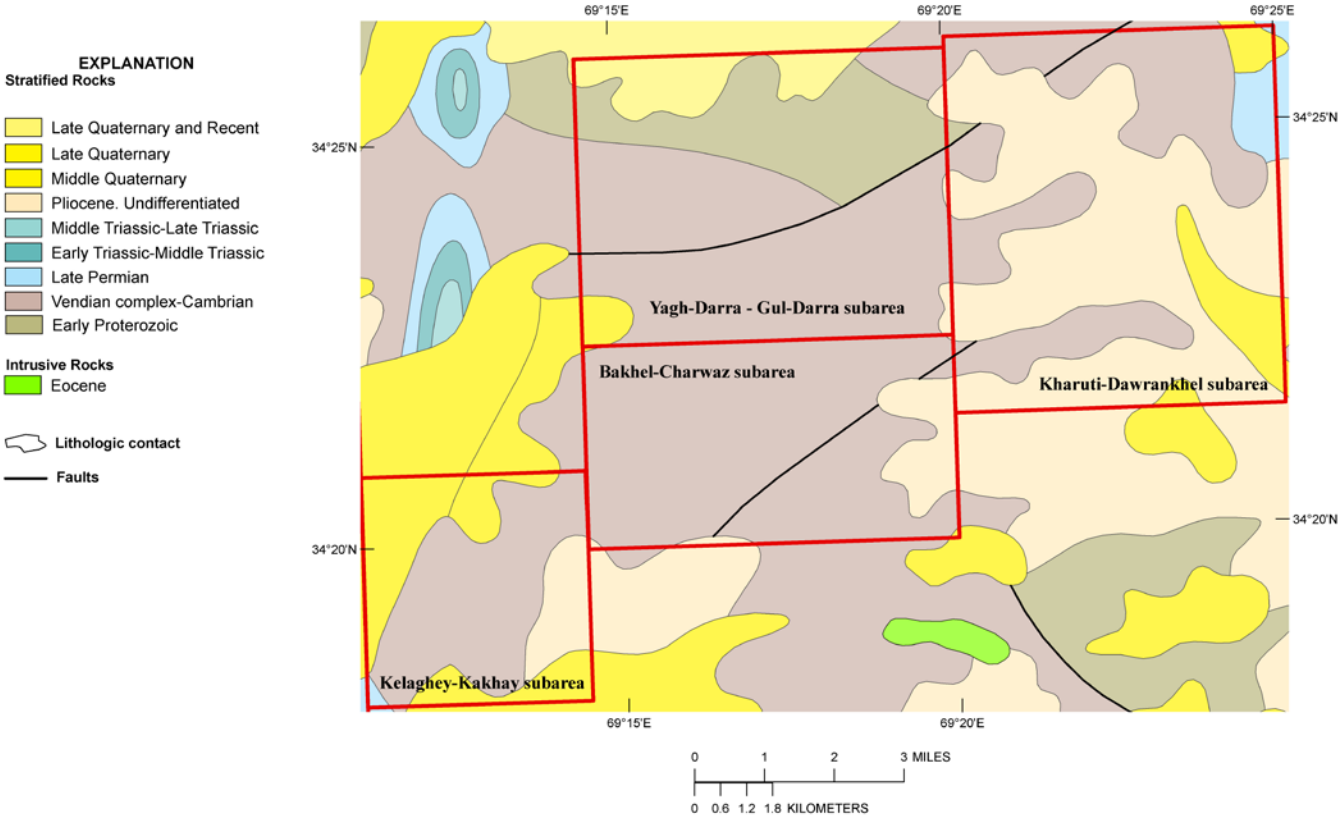

Figure 2B–15. Geologic map of the Aynak subareas of the Aynak-Logar Valley area of interest from Dronov and others (1972). Subareas: Kelaghey–Kakhay, Bakhel–Charwaz, Yagh-Darra–Gul-Darra, and Kharuti–Dawrankhel.

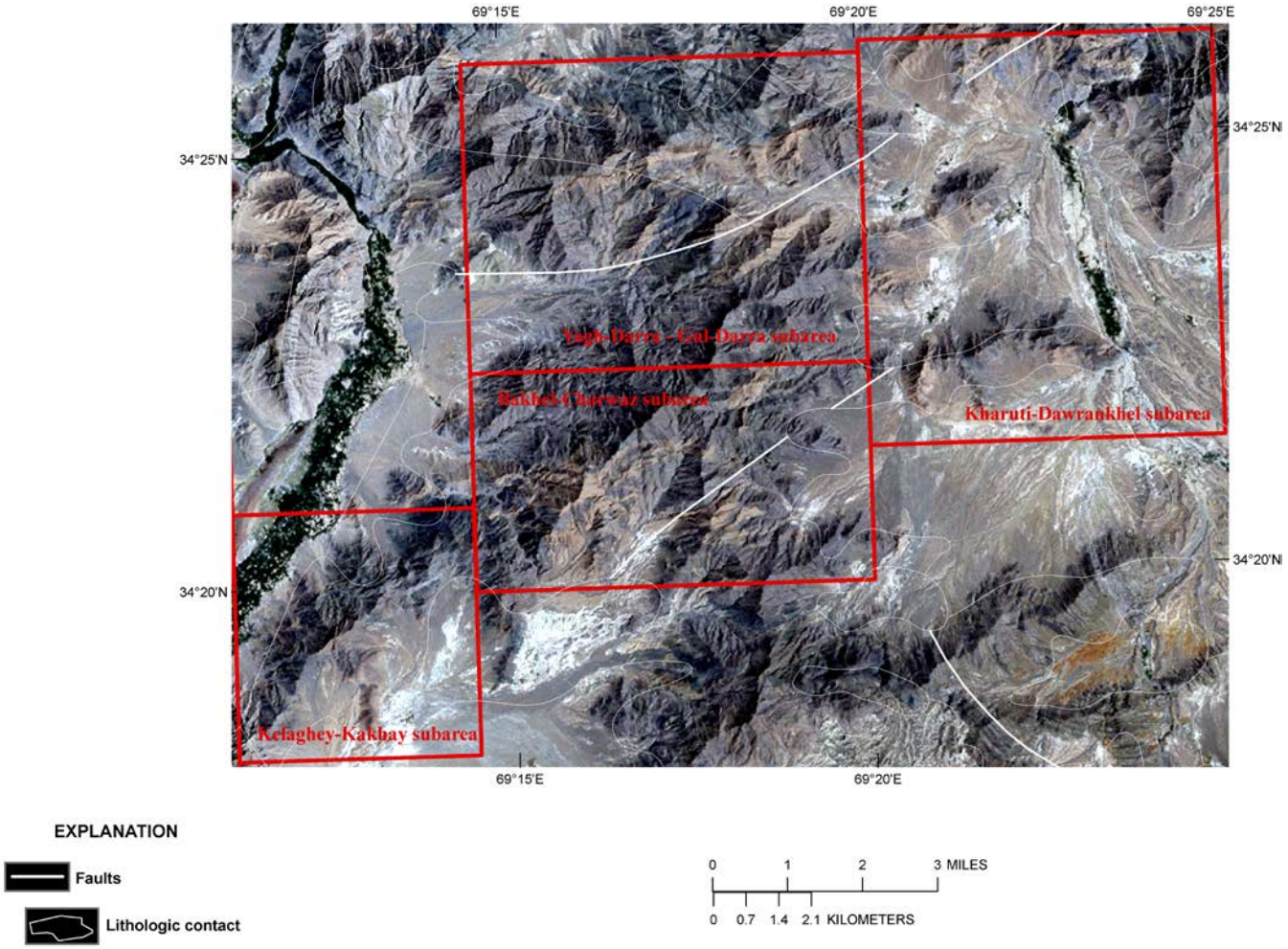

Figure 2B–16. Numerous faults and fractures of different orientations and extent occur in the Aynak subareas of the Aynak-Logar Valley area of interest. The fault traces (Peters and others, 2007) are placed on a Landsat Thematic Mapper (TM) image (Davis, 2007). Marked color differences in the TM data are associated with rocks of different ages. Light pink-brown dolomite rich lenses are seen throughout the middle two (Yagh-Darra–Gul-Darra, and Bakhel-Charwaz) subareas.

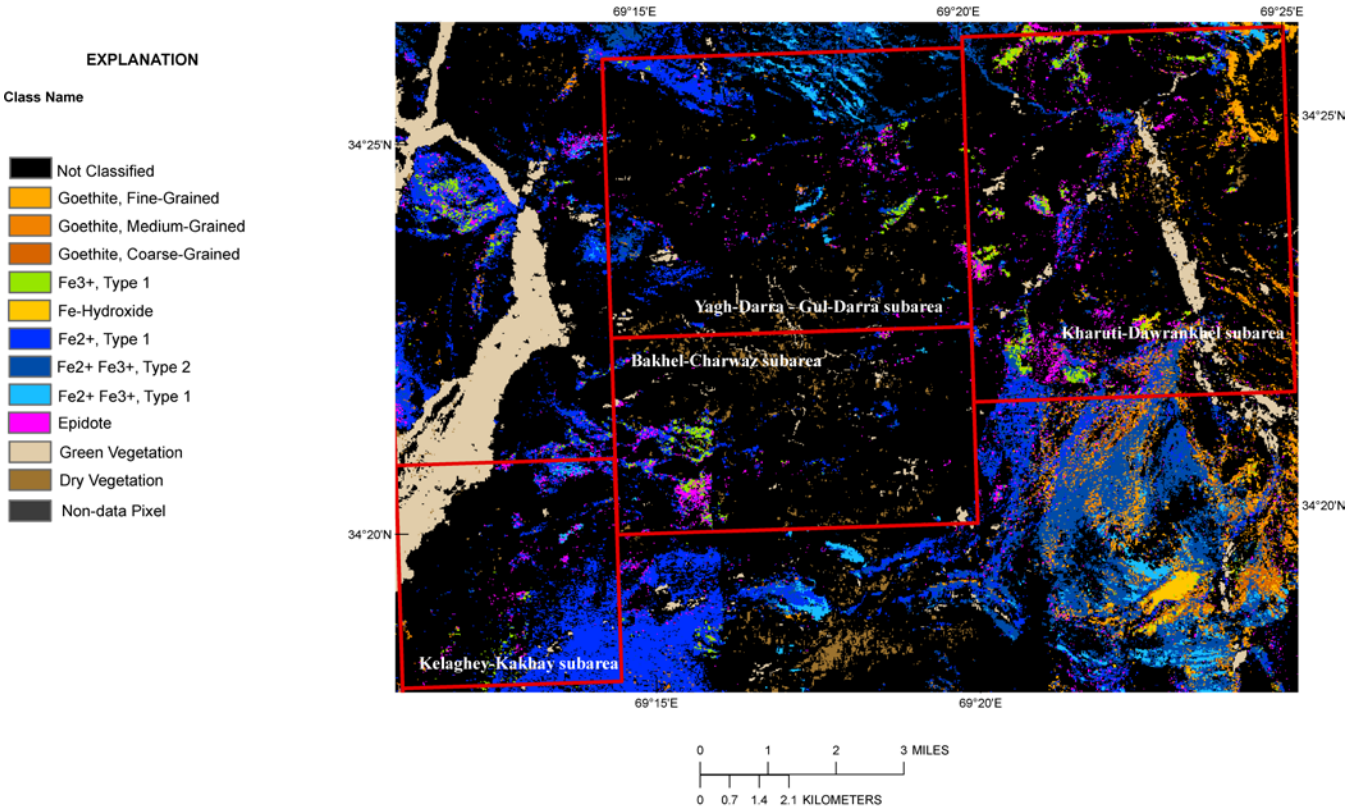

Figure 2B–17. Iron-bearing and other alteration minerals detected in the HyMap data for the Aynak subareas of the Aynak-Logar Valley area of interest are shown in this image. Subareas: Kelaghey-Kakhay, Bakhel-Charwaz, Yagh-Darra–Gul-Darra, and Kharuti-Dawrankhel .

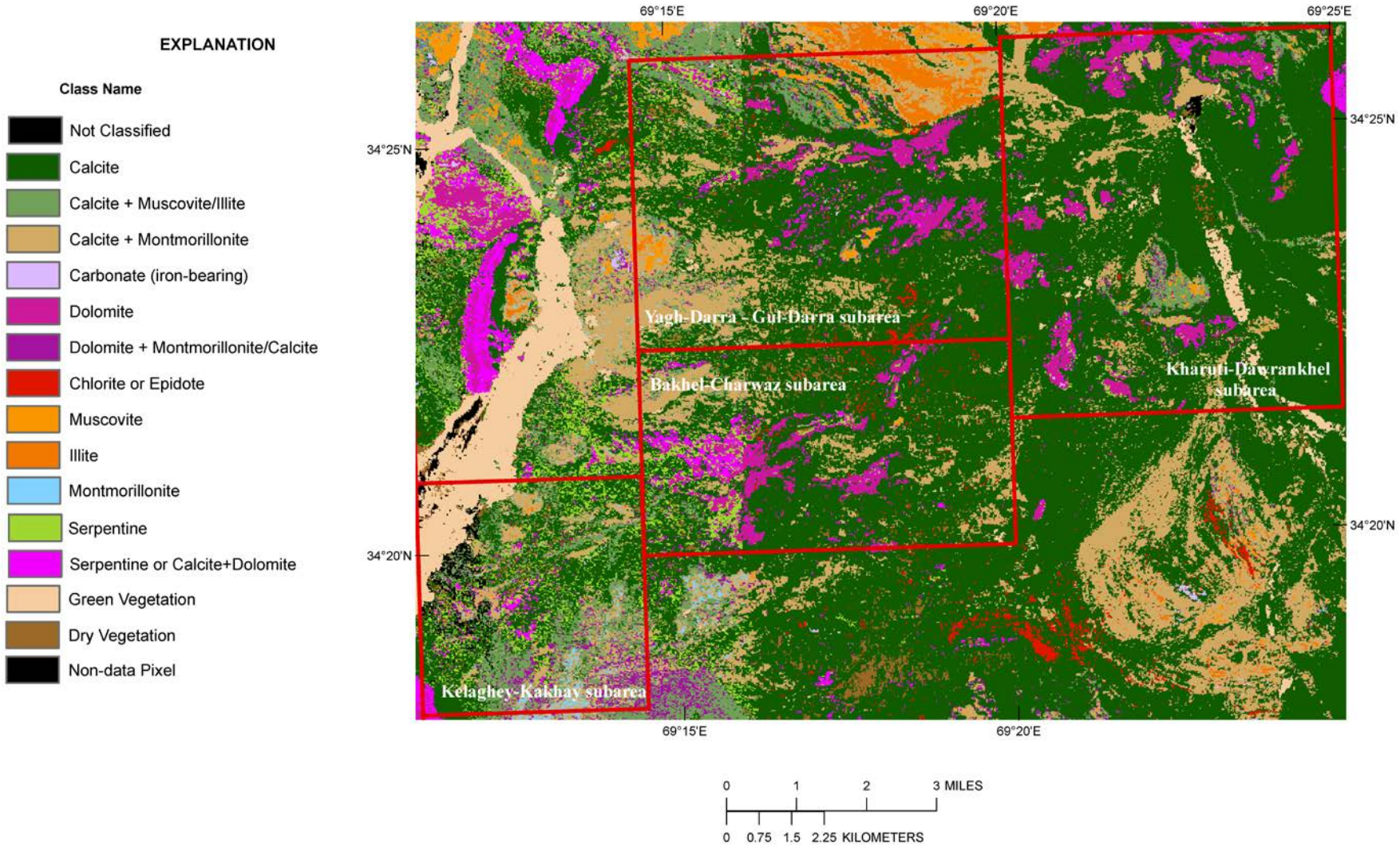

Figure 2B–18. Distribution of clays, carbonates, phyllosilicates, sulfates, altered minerals, and other materials for the Aynak subareas of the Aynak-Logar Valley area of interest based on the HyMap data. Subareas: Kelaghey–Kakhay, Bakhel–Charwaz, Yagh-Darra–Gul-Darra, and Kharuti–Dawrankhel.

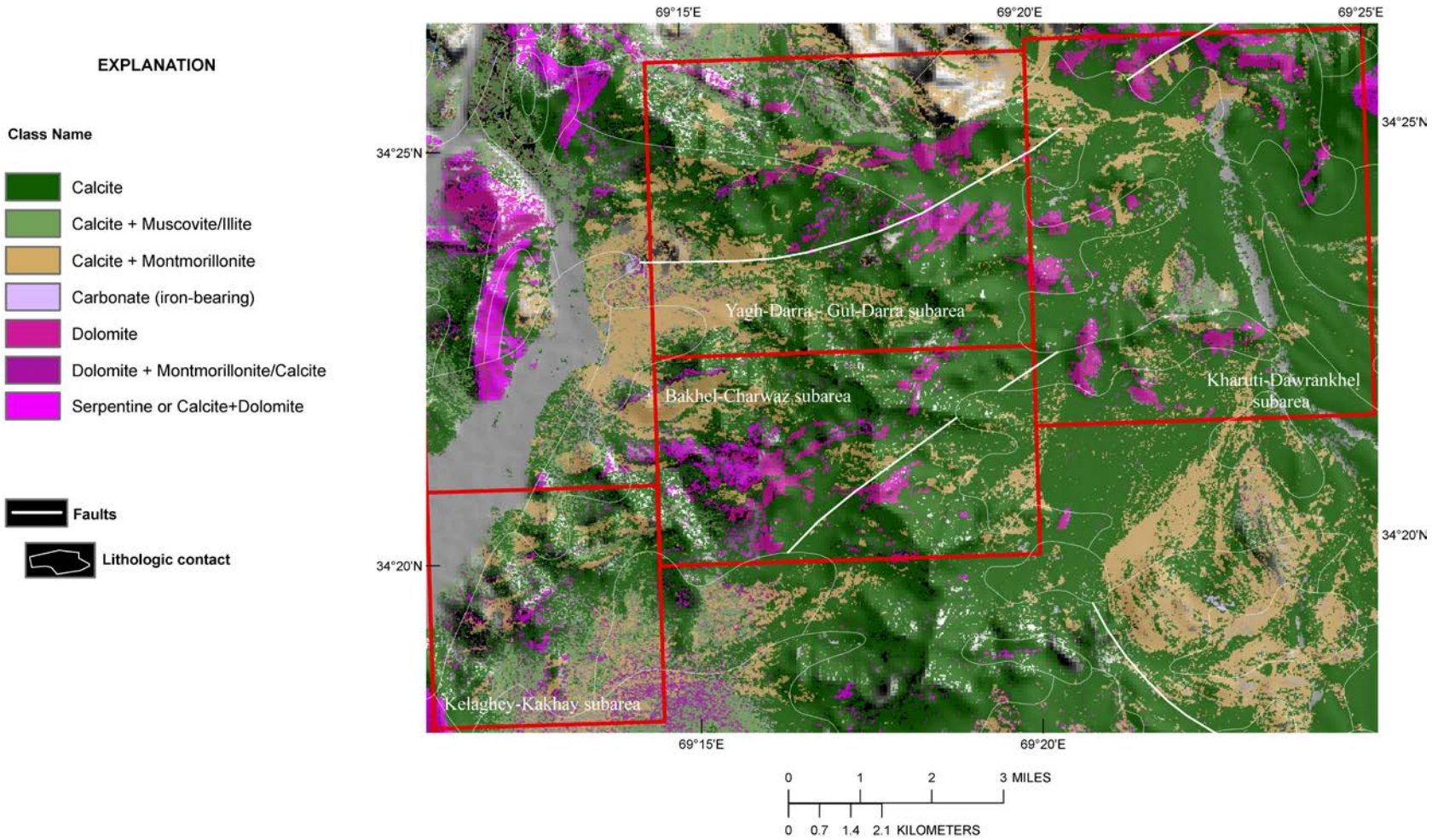

Figure 2B–19. Distribution of carbonate-bearing minerals in the Aynak subareas detected in the HyMap data. Subareas: Kelaghey–Kakhay, Bakhel–Charwaz, Yagh-Darra–Gul-Darra, and Kharuti–Dawrankhel.

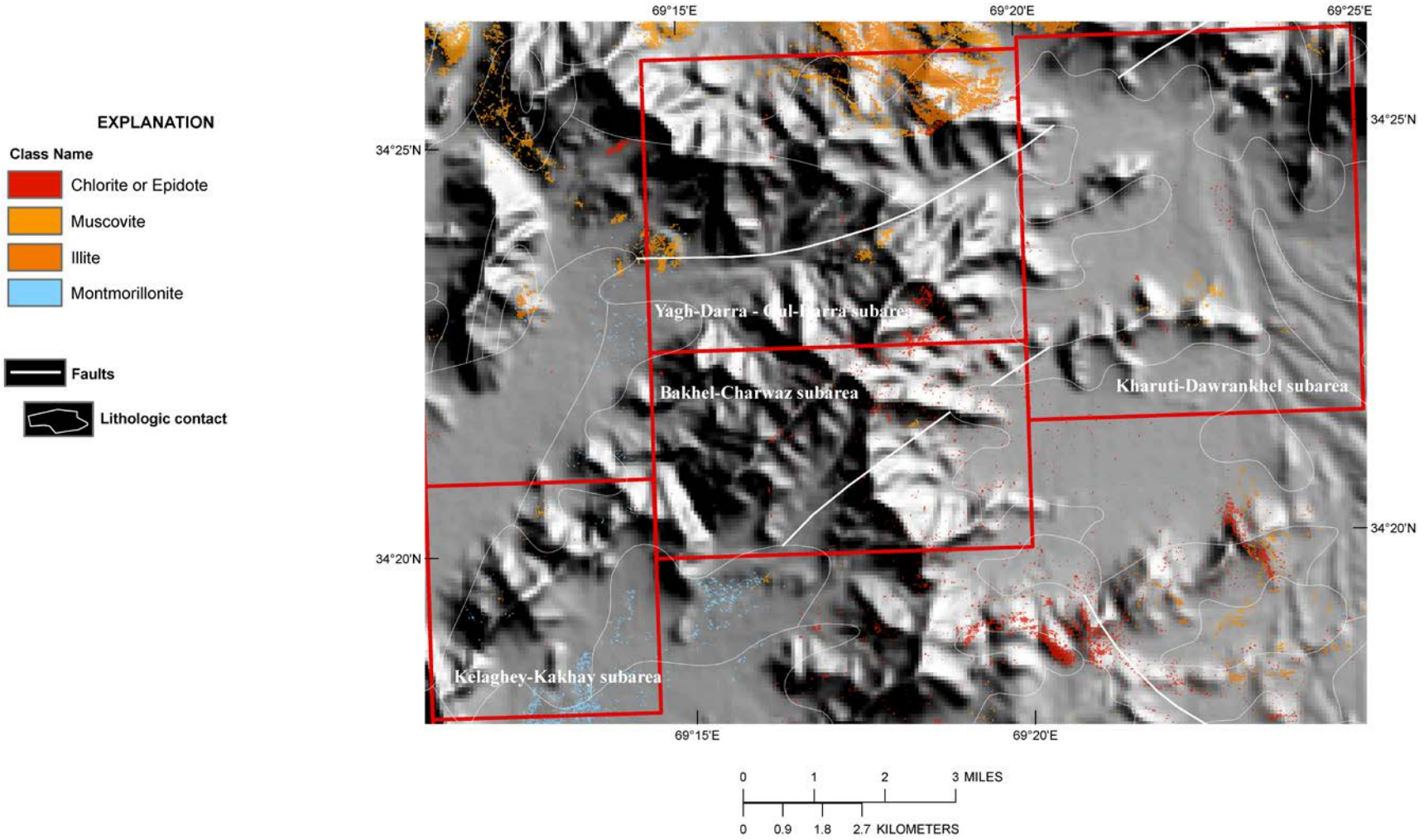

Figure 2B–20. Distribution of clays and micas detected using the HyMap data. Subareas: Kelaghey–Kakhay, Bakhel–Charwaz, Yagh-Darra–Gul-Darra, and Kharuti–Dawrankhel.

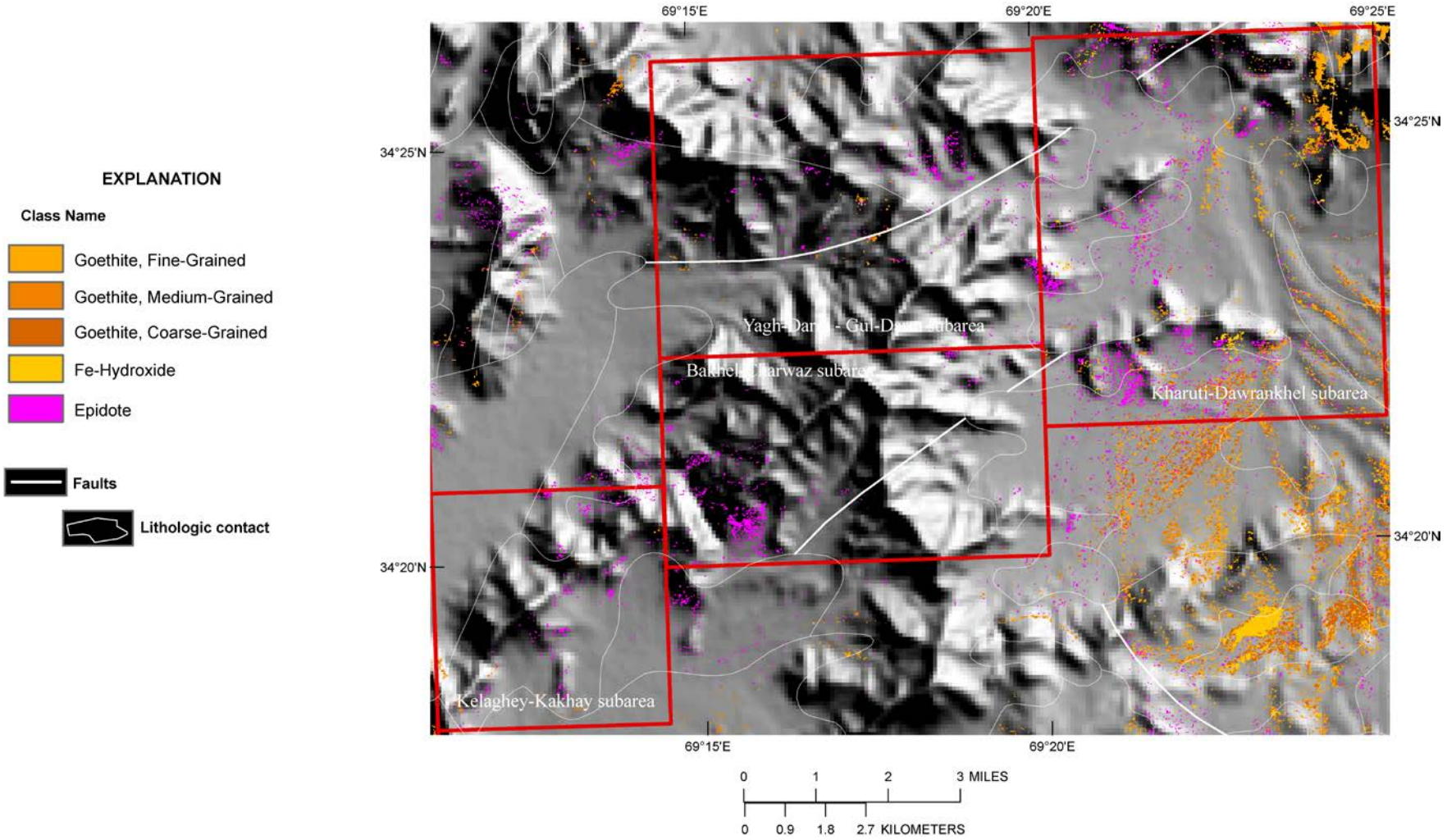

Figure 2B–21. Distribution of Iron-hydroxides and Iron-oxides for the Aynak subareas. Subareas: Kelaghey–Kakhay, Bakhel–Charwaz, Yagh-Darra–Gul-Darra, and Kharuti–Dawrankhel.

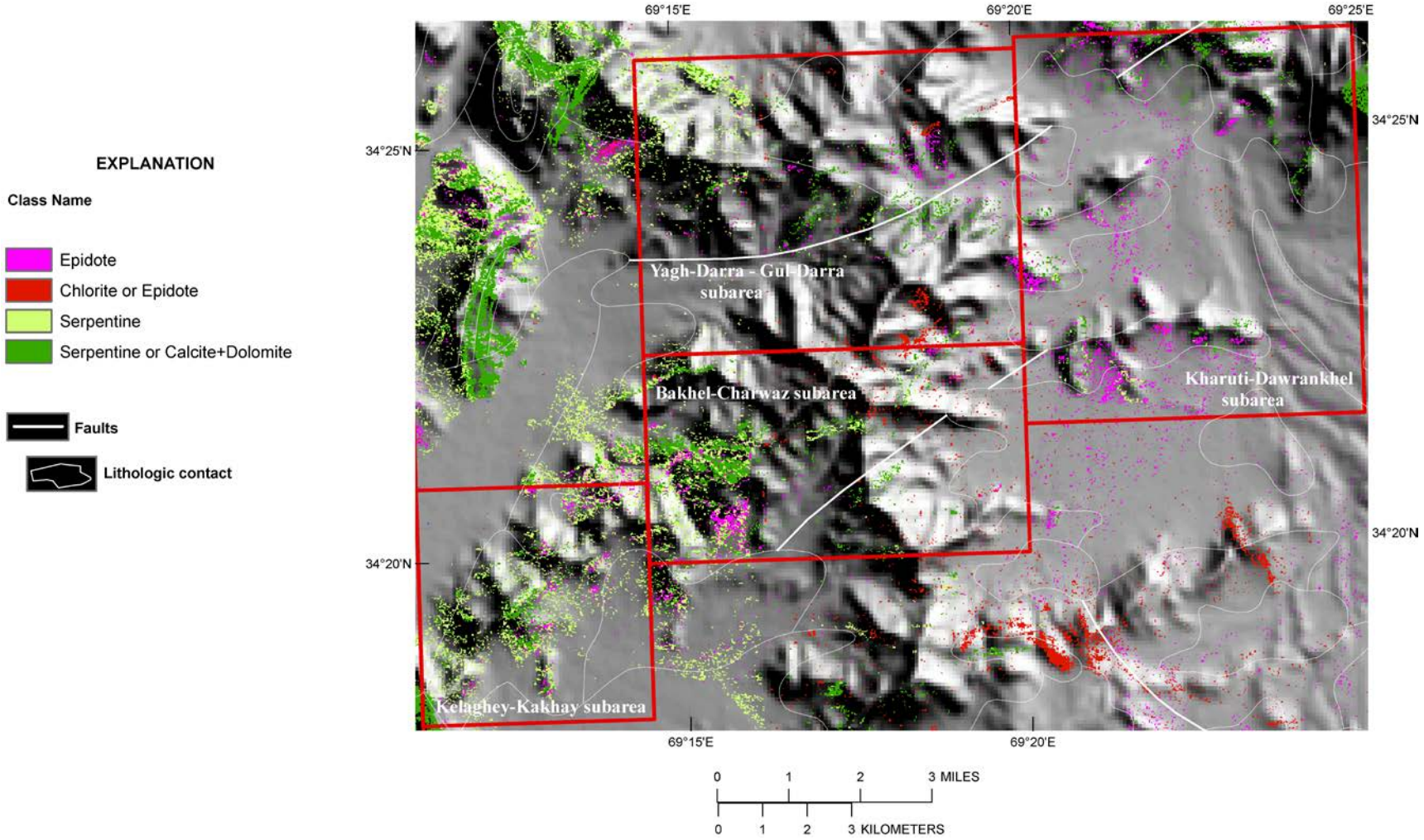

Figure 2B–22. Distribution of common secondary minerals detected in the HyMap data. Subareas: Kelaghey–Kakhay, Bakhel–Charwaz, Yagh-Darra–Gul-Darra, and Kharuti–Dawrankhel.

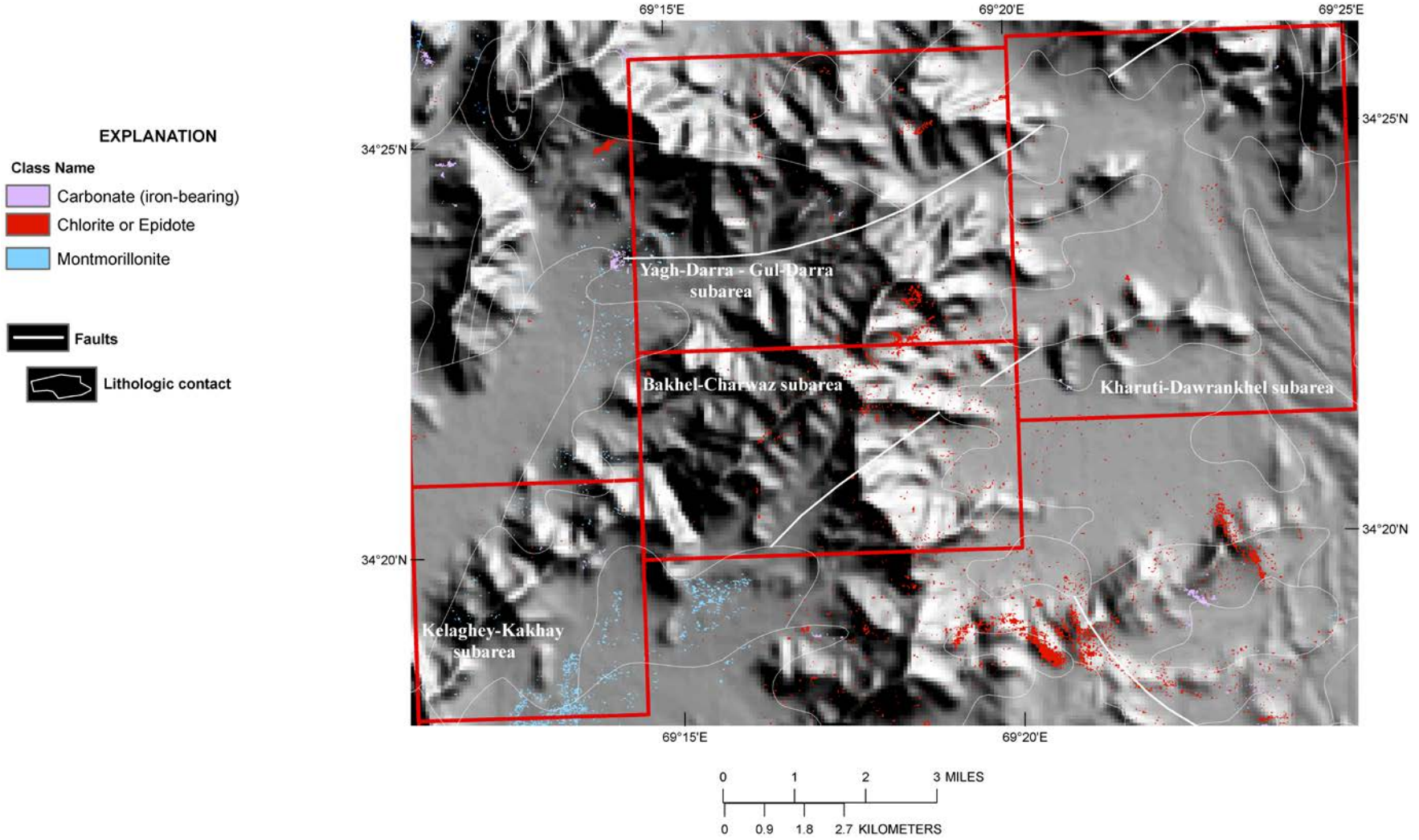

Figure 2B–23. Common alteration materials detected in the HyMap data. Subareas: Kelaghey–Kakhay, Bakhel–Charwaz, Yagh-Darra–Gul-Darra, and Kharuti–Dawrankhel.

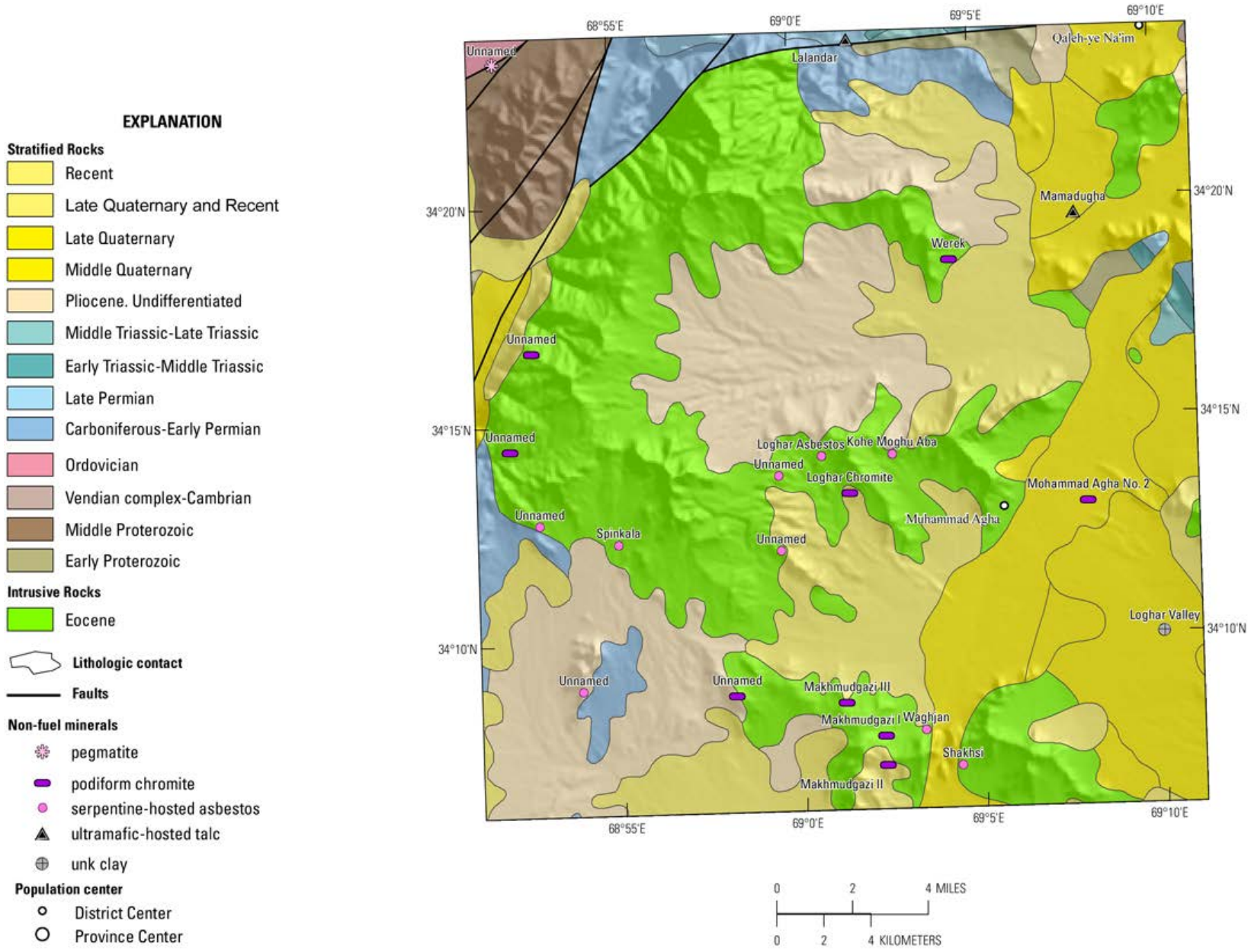

Figure 2B–24. Known mineral occurrences in the Logar Valley subarea of the Aynak-Logar Valley area of interest. Unk, unknown.

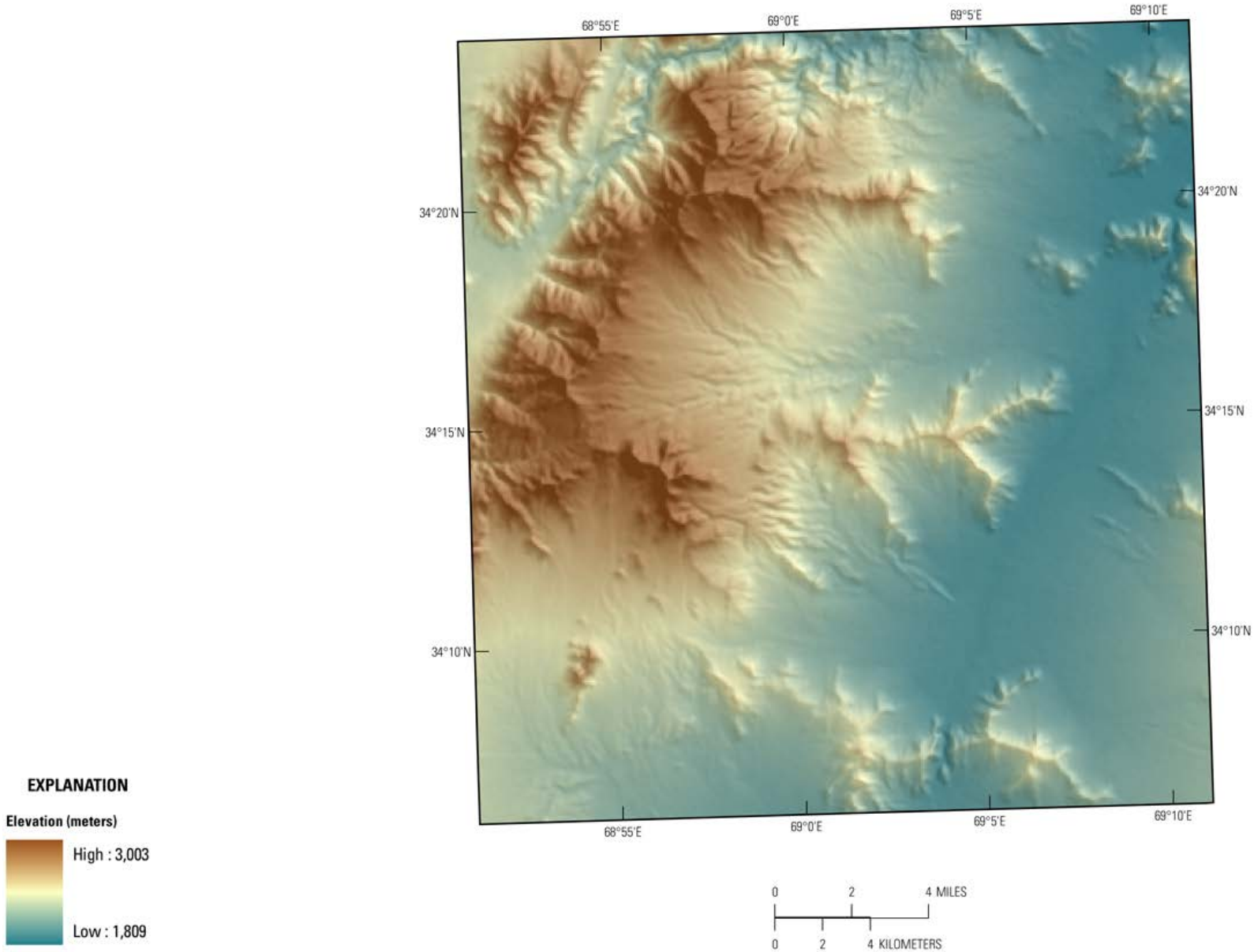

Figure 2B–25. Shaded-relief map showing the elevation of the Logar Valley. The darker brown tones indicate the higher elevations and the lower elevations are represented by the blue tones.

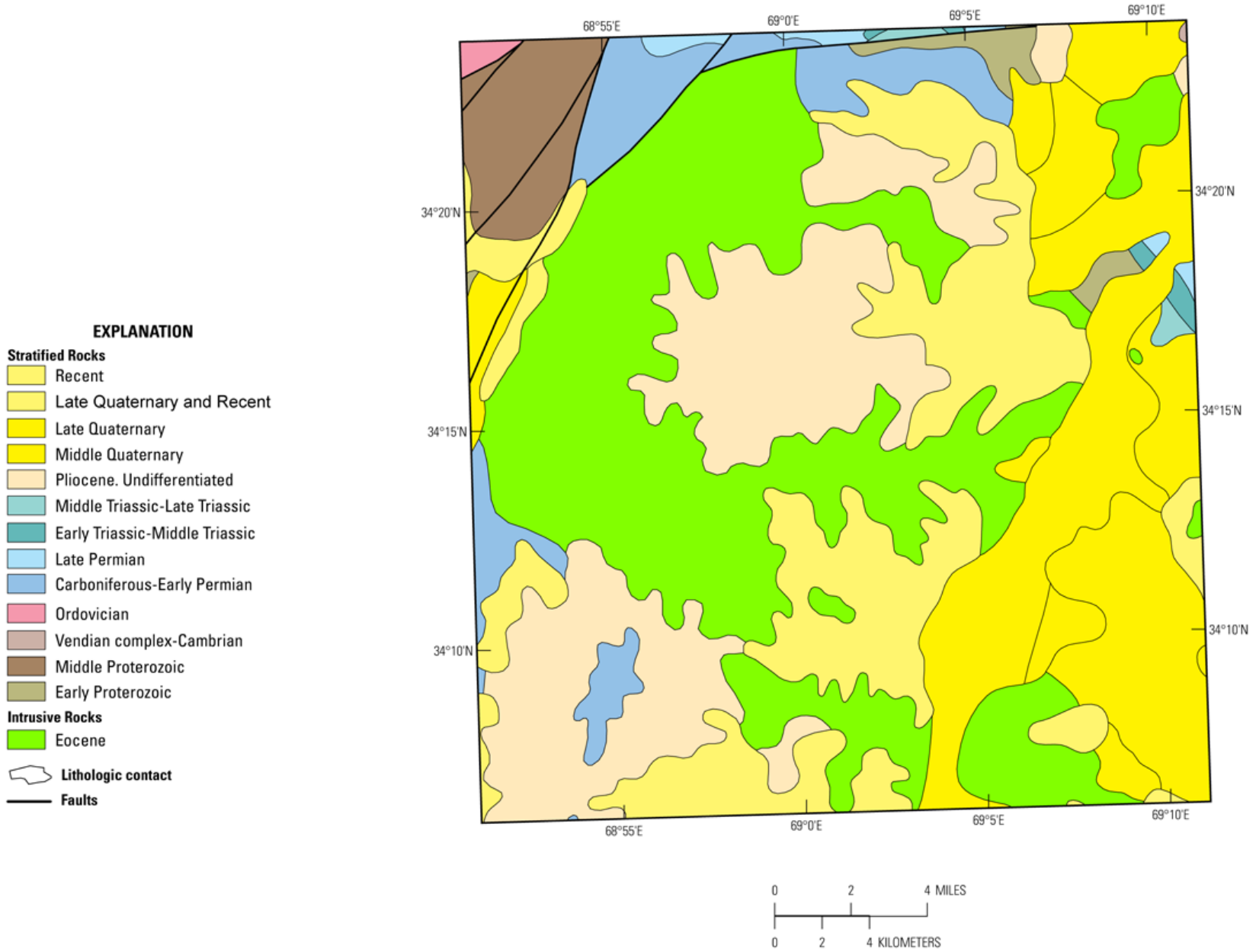

Figure 2B–26. Geologic map of the Logar Valley subarea of the Aynak-Logar Valley area of interest taken from Dronov and others (1972).

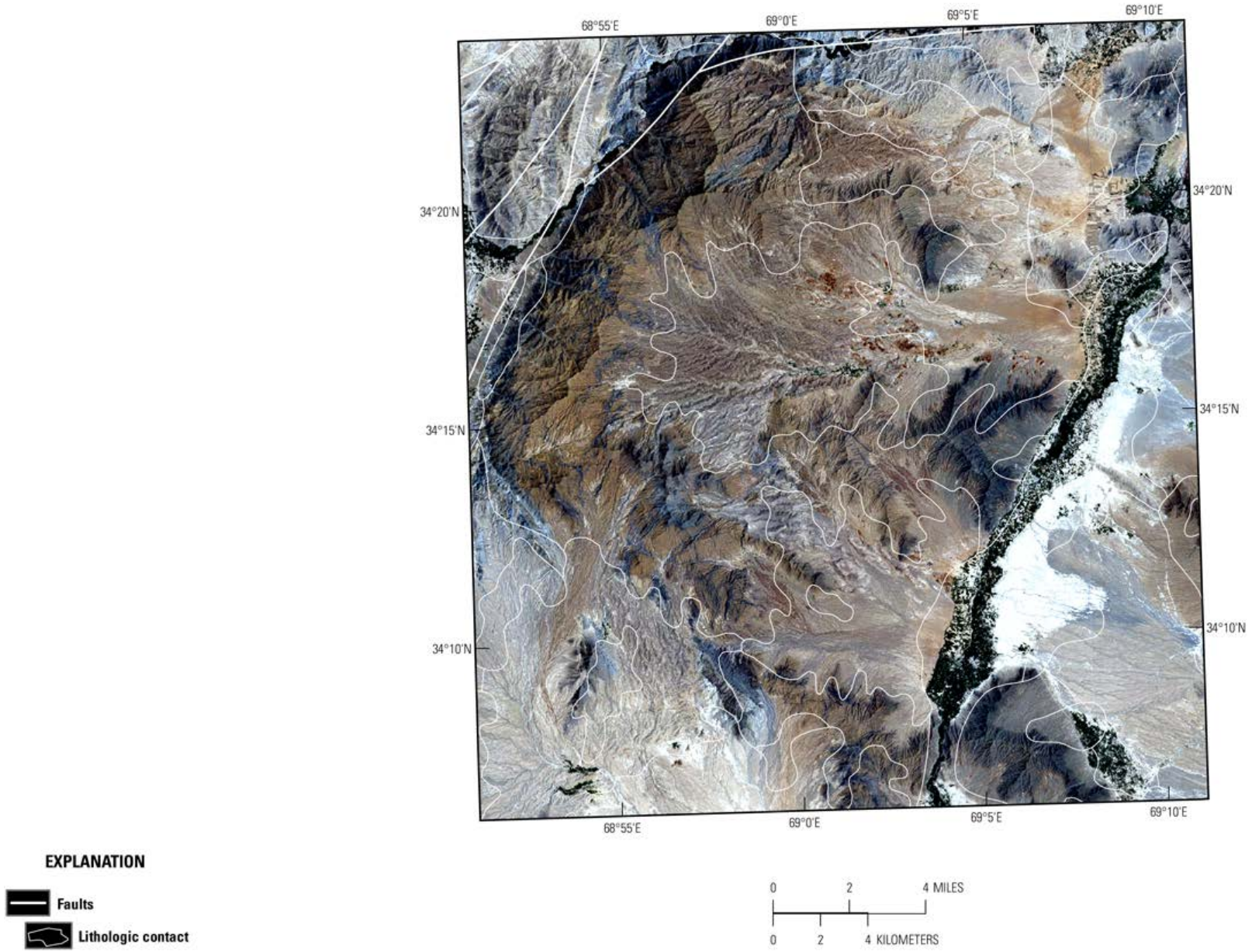

Figure 2B–27. Landsat Thematic Mapper (TM) image of the Logar Valley subarea. Fault traces (Peters and others, 2007) are placed on the Landsat TM image (Davis, 2007). Color difference in the TM data correlate with different geologic units.

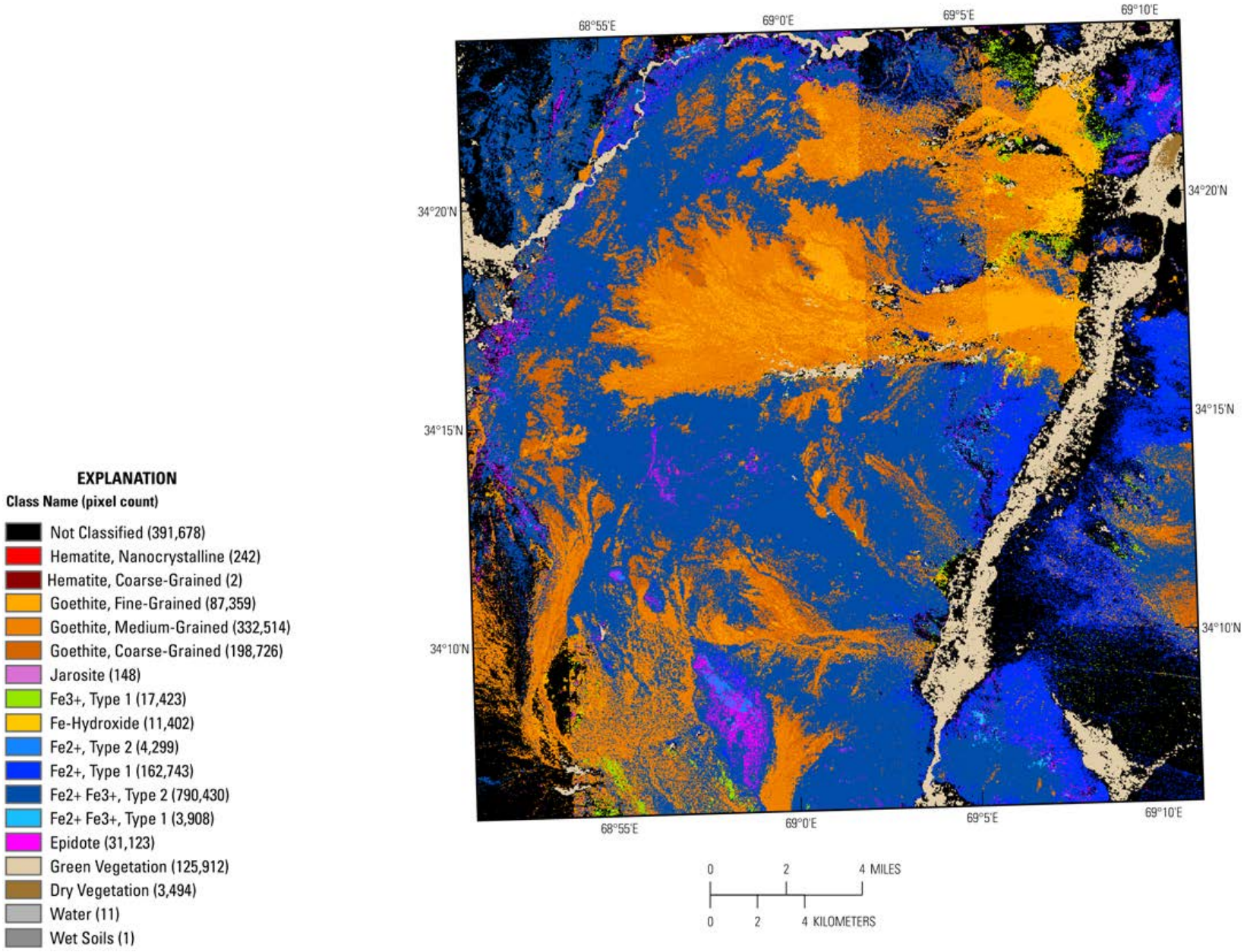

Figure 2B–28. Iron-bearing and other alteration minerals detected in the HyMap data of the Logar Valley subarea.

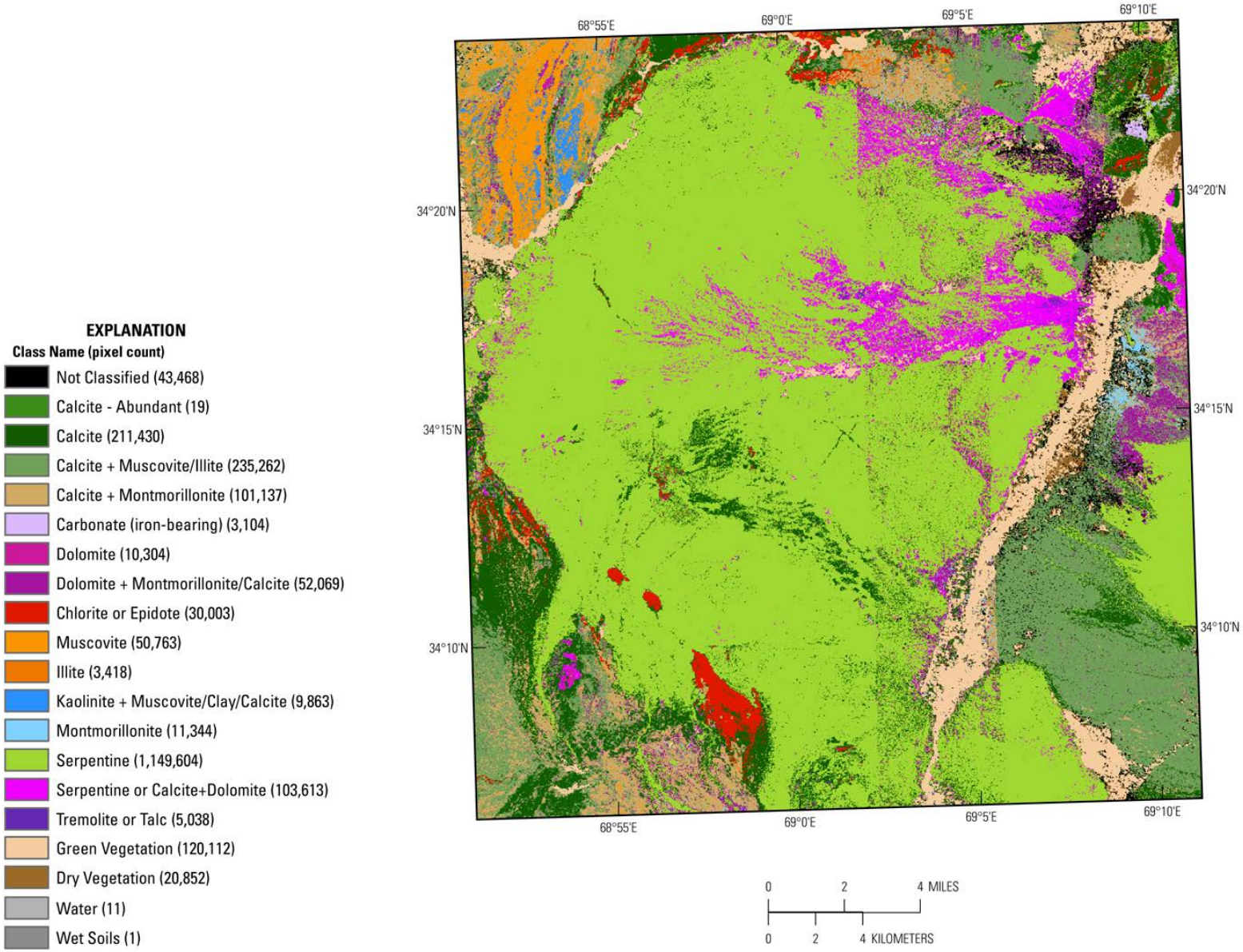

Figure 2B–29. Distribution of clays, carbonates, phyllosilicates, sulfates, altered minerals, and other materials for the Logar Valley subarea of the Aynak-Logar Valley area of interest using the HyMap data.

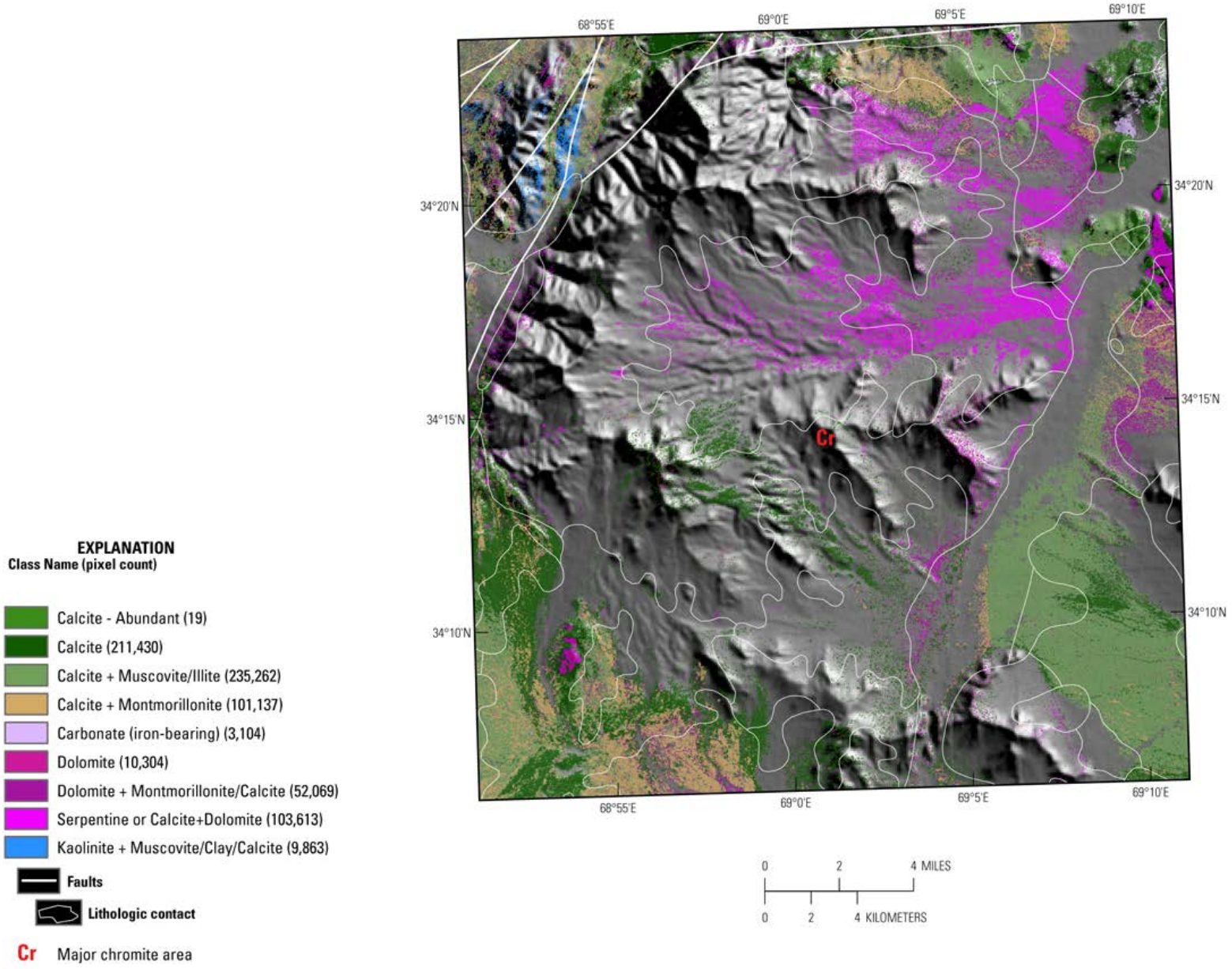

Figure 2B–30. Distribution of carbonate-bearing minerals in the Logar Valley subarea detected in the HyMap data.

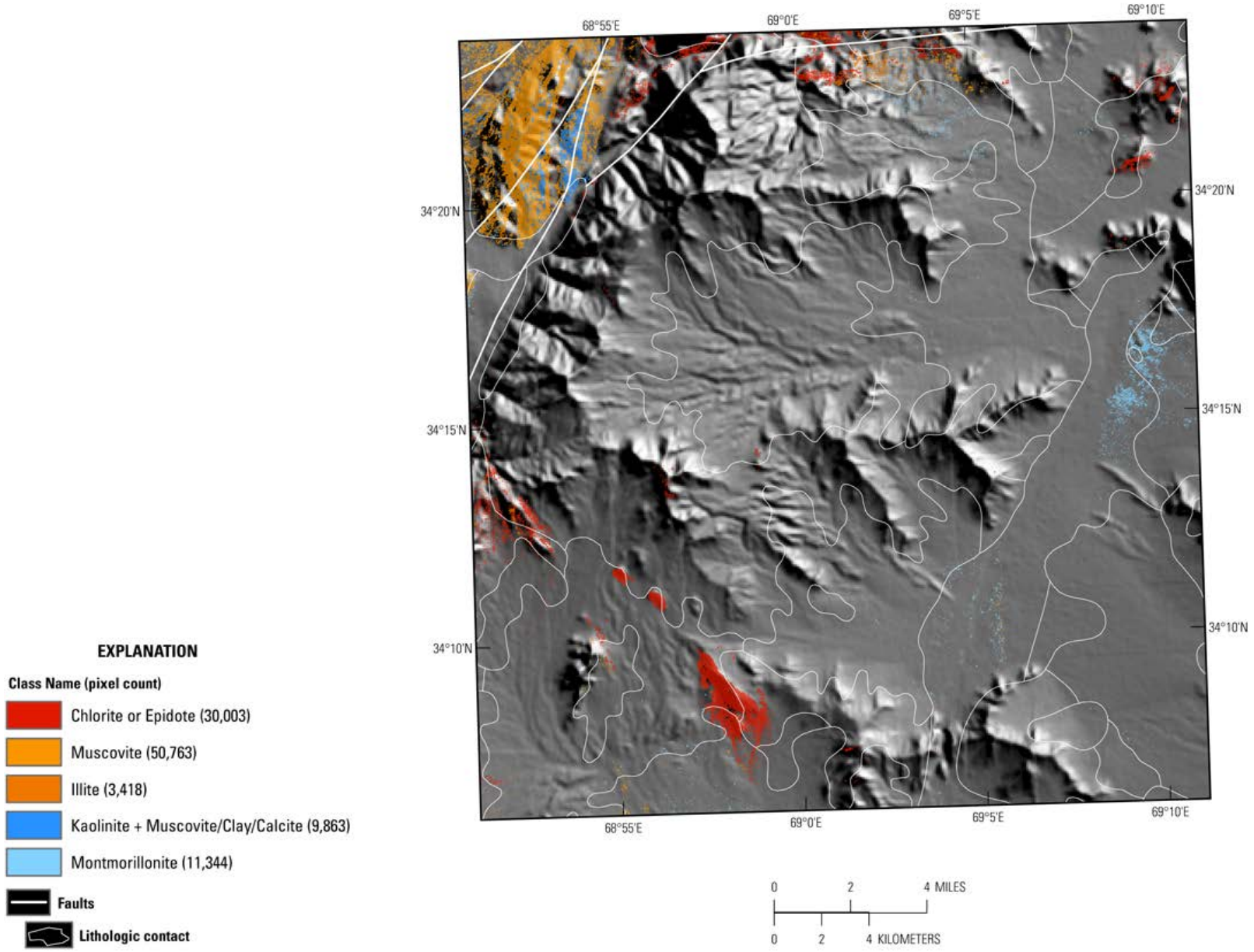

Figure 2B–31. Distribution of clays and micas in the Logar Valley subarea that were mapped using the HyMap data.

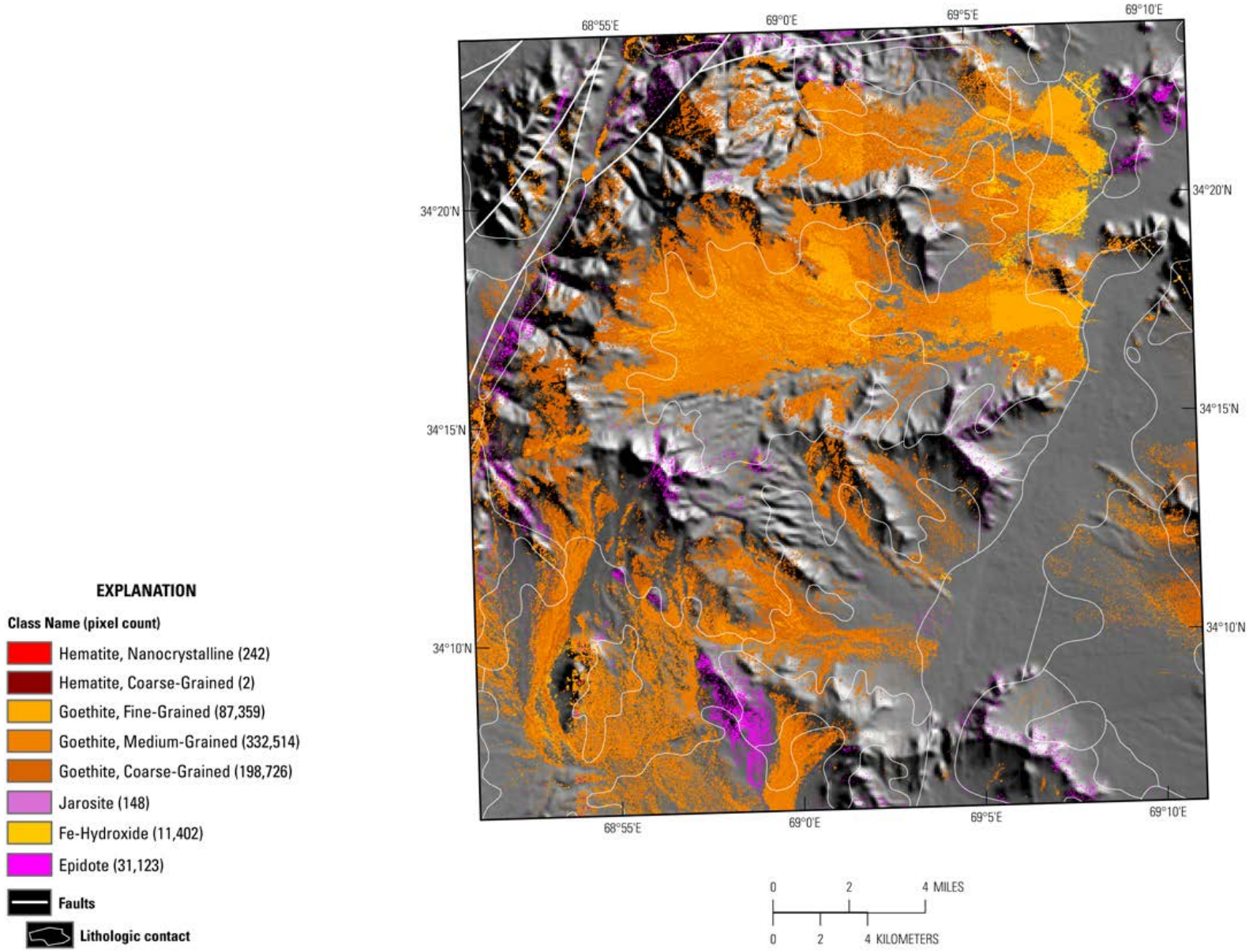

Figure 2B–32. Distribution of iron-hydroxides, iron-oxides, and other minerals for the Logar Valley subarea.

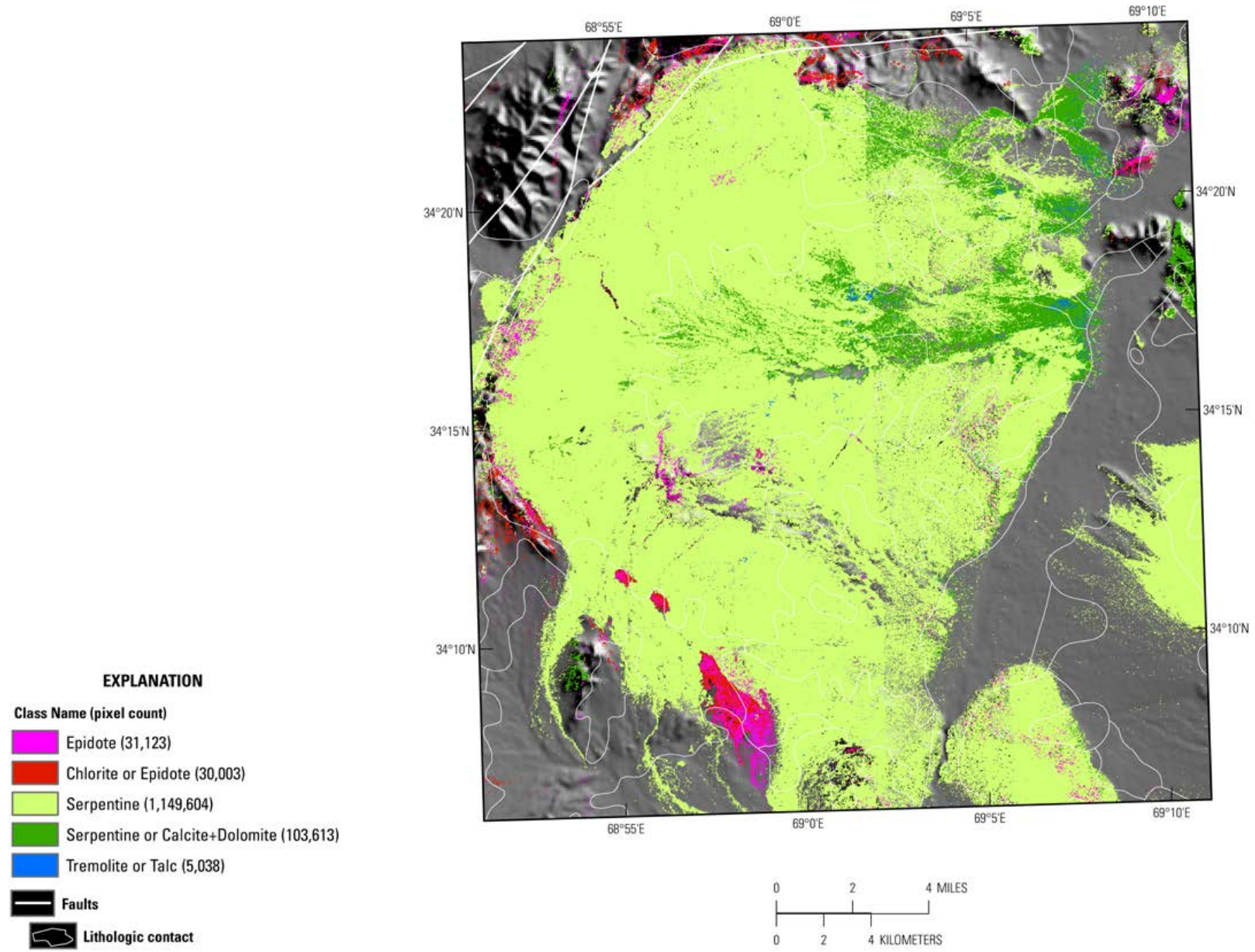

Figure 2B–33. Common secondary minerals detected in the HyMap data for the Logar Valley subarea of the Aynak-Logar Valley area of interest.

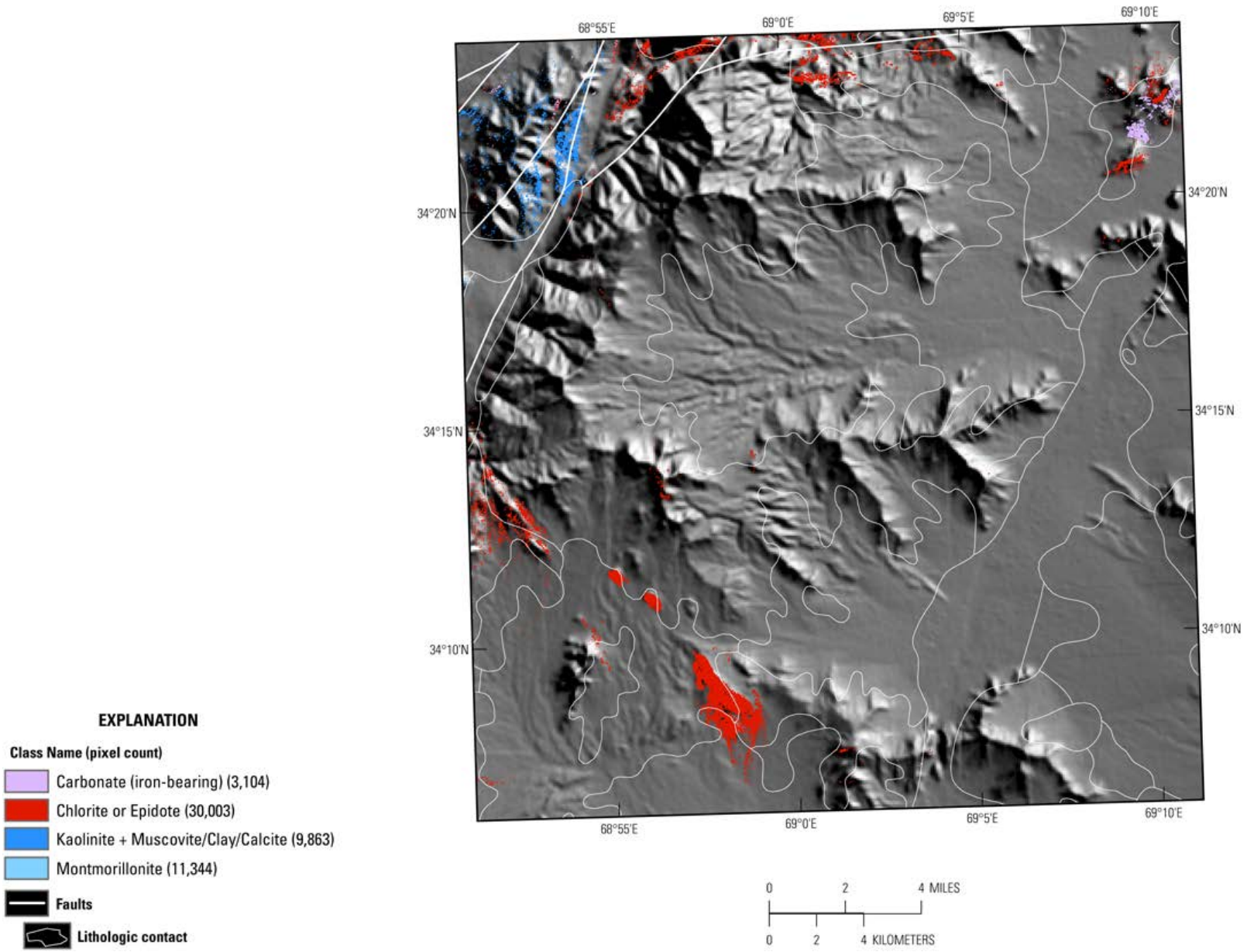

Figure 2B–34. Common alteration materials detected in the HyMap data are shown on this map.

2B.4 Summary

Mineral maps created using image spectrometer data show lithologic, structural, and surface process details within the region of interest. Lithologically and structurally, three major terranes are mapped: the layered metasedimentary Aynak subareas on the east, the massive blocks containing ultramafic rock within Logar Valley in the center, and the faulted and highly contorted bedding within the Paghman area on the west. Lithologic units can be traced by their mineralogy that shows folding, faulting, and stratigraphic variations. Surface processes, such as mineral weathering and erosion, are also shown by the distribution of clays, iron oxides, carbonates, and micas.

The Aynak subareas contain abundant calcite with clay and mica, with lenses and pods of dolomite-rich rock that trend with copper mineralization and topography. An association may exist with igneous porphyries, but the exact relation is unclear. Low abundances of mapped iron-bearing minerals occur within the metasedimentary rock, but chlorite and (or) epidote is associated with field-mapped amphibole occurrence within the Welayati Formation. Muscovite is spectrally mapped within older gneisses on the northern boundary.

The Logar Valley subarea shows widespread serpentine with ferrous- and ferric-iron minerals within the country rock. Additional spectrally detected minerals include chlorite and (or) epidote mapped on the north and south contacts of the ultramafic rocks with Paleozoic carbonates and a band of calcite that occurs near known chromite mineralization. The calcite band in the ultramafics is possibly related to serpentine altering to carbonate minerals.

The present analysis suggests that chromite may be targeted for detailed spectroscopic analysis tailored to identify it and specific carbonate phases. Also, the Welayati, Loy Khwar, and Gulkhamid Formations, which host copper mineralization, may be spectrally identified in more detail with additional work.

2B.5 References Cited

Abdullah, Sh., and Chmyriov, V.M., 1977, Geological map of Afghanistan: Kabul, Afghanistan, Ministry of Mining and Industry of Democratic Republic of Afghanistan, scale 1:500,000.

Abdullah, Sh., Chmyriov, V.M., Stazhilo-Alekseev, K.F., Dronov, V.I., Gannan, P.J., Rossovskiy, L.N., Kafarskiy, A.Kh., and Malyarov, E.P., 1977, Mineral resources of Afghanistan (2d edition): Kabul, Afghanistan, Republic of Afghanistan Geological and Mineral Survey, 419 p.

Bohannon, R.G., 2010, Geologic and topographic maps of the Kabul South 30′ × 60′ quadrangle, Afghanistan: U.S. Geological Survey Scientific Investigations Map 3137, scale, 1:100,000.

Clark, R.N., Swayze, G.A., Livo, K.E., Kokaly, R.F., King, T.V.V., Dalton, J.B., Vance, J.S., Rockwell, B.W., Hoefen, T., and McDougal, R.R., 2003a, Surface reflectance calibration of terrestrial imaging spectroscopy data—A tutorial using AVIRIS, *in* Green, R.O., ed., Proceedings of the 11th JPL Airborne Earth Science Workshop: JPL Publication 03-4, p. 43–63.

Clark, R.N., Swayze, G.A., Livo, K.E., Kokaly, R.F., Sutley, S.J., Dalton, S.J., McDougal, R.R., and Gent, C.A., 2003b, Imaging spectroscopy—Earth and planetary remote sensing with the USGS Tetracorder and Expert Systems: Journal of Geophysical Research, v. 108, no. E12, 5131, 44 p. DOI:10.1029/2002JE001847.

Cocks T., Jenssen, R., Stewart, A., Wilson, I., and Shields, T. 1998, The HyMap airborne hyperspectral sensor—The system, calibration and performance, in Schaepman, M., Schlapfer, D., and Itten, K.I., eds., Proceedings of the 1st EARSeL Workshop on Imaging Spectroscopy, 6–8 October 1998, Zurich: Paris, European Association of Remote Sensing Laboratories, p. 37–43.

Davis, P.A., 2007, Landsat ETM+ false-color image mosaics of Afghanistan: U.S. Geological Survey Open-File Report 2007–1029, 22 p.

Doebrich, J.L., and Wahl, R.R., comps., *with contributions by* Doebrich, J.L., Wahl, R.R., Ludington, S.D., Chirico, P.G., Wandrey, C.J., Bohannon, R.G., Orris, G.J., Bliss, J.D., and _____, 2006, Geologic and mineral resource map of Afghanistan: U.S. Geological Survey Open File Report 2006–1038, scale 1:850,000, available at *http://pubs.usgs.gov/of/2006/1038/*.

Dronov, V.I., Kalimulin, S.M., Sborshchikov, I.M., Svezhentsov, V.P., Chistyakov, A.N., Zelensky, E.D., and Cherepov, P.G., 1972, The geology and minerals of North Afghanistan (parts of map sheets 400-II and 500-I, the Kaysar-Hari Rod Interfluve area): [Afghanistan] Department of Geological and Mineral Survey, 44 p.

Hoefen, T.M., Kokaly, R.F., and King, T.V.V., 2010, Calibration of HyMap data covering the country of Afghanistan, *in* Proceedings of the 15th Australasian Remote Sensing and Photogrammetry Conference, Alice Springs, Australia, September 12–17, 2010, p. 409, available at *http://dl.dropbox.com/u/81114/15ARSPC-Proceedings.zip/*.

King, T.V.V., Johnson, M.R., Hoefen, T.M., Kokaly, R.F., and Livo, K.E., 2011, Mapping potential mineral resource anomalies using HyMap data, *in* King, T.V.V., Johnson, M.R., Hubbard, B.E., and Drenth, B.J., eds, Identification of mineral resources in Afghanistan—Detecting and mapping resource anomalies in prioritized areas using geophysical and remote sensing (ASTER and HyMap) data in Afghanistan: U.S. Geological Survey Open-File Report 2011–1229, available at *http://pubs.usgs.gov/of/2011/1229/*.

King, T.V.V., Kokaly, R.F., Hoefen, T.M., and Knepper, D.H., 2010, Resource mapping in Afghanistan using HyMap data, *in* Proceedings 15th Australasian Remote Sensing and Photogrammetry Conference, Alice Springs, Australia, September 12–17, 2010, p. 500.

King, T.V.V., Kokaly, R.F., Hoefen, T.M., Dudek, K. and Livo, K.E., 2011, Surface materials map of Afghanistan—Iron-bearing minerals and other materials: U.S. Geological Survey Scientific Investigations Map 3152–B.

Kokaly, Ray, 2011, PRISM—Processing routines in IDL for spectroscopic measurements: U.S. Geological Survey Open-File Report 2011–1155, available at *http://pubs.usgs.gov/of/2011/1155/*.

Kokaly, R.F., King, T.V.V., and Livo, K.E., 2008, Airborne hyperspectral survey of Afghanistan, 2007: Flight line planning and HyMap data collection: U.S. Geological Survey Open-File Report 2008–1235, 14 p.

Kokaly, R.F., King, T.V.V., Hoefen, T.M., Dudek, K. and Livo, K.E., 2011, Surface materials map of Afghanistan—Carbonates, phyllosilicates, sulfates, altered minerals, and other materials: U.S. Geological Survey Scientific Investigations Map SIM 3152–A.

Peters, S.G., Ludington, S.D., Orris, G.J., Sutphin, D.M., Bliss, J.D., and Rytuba, J.J., eds., and the U.S. Geological Survey-Afghanistan Ministry of Mines Joint Mineral Resource Assessment Team, 2007, Preliminary non-fuel mineral resource assessment of Afghanistan: U.S. Geological Survey Open-File Report 2007–1214, 810 p., 1 CD–ROM. (Also available at *http://pubs.usgs.gov/of/2007/1214/*.)

Tapponier, P., Mattauer, M., Proust, F., and Cassaigneau, C., 1981, Mesozoic ophiolites, sutures, and large-scale tectonic movements in Afghanistan: Earth and Planetary Science Letters, v. 52, no. 2, p. 355–371.

Volin, M.E., 1950, Chromite deposits of Logar Valley, Kabul Province, Afghanistan: Washington, D.C., U.S. Bureau of Mines Report, 58 p.